Pesquisas em Geociências

v. 51, nº 3 (2024)
doi.org/10.22456/1807-9806.137240

Research Paper

The Impact of Diagenetic Processes on the Quality of Carbonate Reservoirs in the Quissamã Formation (Albian), Tubarão Azul Field, Campos Basin, Brazil

O Impacto dos Processos Diagenéticos Sobre a Qualidade de Reservatórios Carbonáticos da Formação Quissamã (Albiano), Campo de Tubarão Azul, Bacia de Campos, Brasil

Leonardo Halfen[1], José Luís Drummond Alves[1], Gisela de Souza Miranda Almeida[1], Luiz Fernando De Ros[2], Francyne Bochi do Amarante[3]

[1]Universidade Federal do Rio de Janeiro, Departamento de Engenharia Civil (COPPE), Rio de Janeiro, Brasil. leonardohalfen@gmail.com; jalves@lamce.coppe.ufrj.br; gisela.almeida@coc.ufrj.br.
[2]Universidade Federal do Rio Grande do Sul, Departamento de Mineralogia e Petrologia, Porto Alegre, Brasil. lfderos@inf.ufrgs.br.
[3]Universidade Federal do Rio Grande do Sul, Programa de Pós-Graduação em Geociências, Porto Alegre, Brasil. fran.bochi@hotmail.com.

Abstract: Albian carbonate reservoirs of the Quissamã Formation have been an important target for oil exploration and production in the Campos Basin for several decades. The variety of depositional facies and the influence of diagenesis in reducing porosity and permeability create great challenges for the exploration and production of these reservoirs. The objective of this study is to identify the main depositional and diagenetic factors that control the porosity and permeability of Albian carbonates in 3-OGX-61-RJS well located in the Tubarão Azul area, southern Campos Basin, through a faciological, petrology and petrophysical integrated analysis. Observed lithofacies include oolitic, oncolitic and peloidal calcarenites, oncolitic and peloidal calcirudites, and hybrid arenites, deposited in a shallow carbonate ramp. The depositional facies were grouped into two facies associations: a high-energy proximal carbonate ramp composed of hybrid sandstones, oncolitic and oolitic calcarenites, and oncolitic calcirudites, and a moderate-energy intermediate carbonate ramp composed of peloidal and oncolitic calcarenites with peloids. The depositional facies were grouped into two facies associations: a high-energy proximal carbonate ramp composed of hybrid arenites, oncolitic and oolitic calcarenites and oncolitic calcirudites, and a moderate-energy intermediate carbonate ramp composed of peloidal and oncolitic calcarenites with peloids. Nine reservoir petrofacies were defined based on the main primary and diagenetic aspects of impact on porosity and permeability. The main observed diagenetic processes were cementation by calcite, replacement by blocky dolomite and pyrite, kaolinite precipitation, mechanical and chemical compaction, including stylolitization, and eodiagenetic and mesodiagenetic dissolution. Early partial cementation by calcite rims and syntaxial growths helped preserve the primary porosity of oolitic and oncolitic calcarenites from the effects of compaction. Interparticle porosity was completely obliterated where eodiagenetic cementation was very intense. Hybrid arenites with little or no early cementation show porosity and permeability extremely reduced by the effects of compaction. These fundamental processes acted directly to control the porosity and permeability of the studied rocks.

Keywords: Diagenesis, Carbonates, Petrography.

Recebido: 12/2023
Aceito: 09/2024
Publicado: 11/2024

Resumo: Os reservatórios carbonáticos albianos da Formação Quissamã têm sido um alvo importante para exploração e produção de petróleo na Bacia de Campos por várias décadas. A variedade de fácies deposicionais e a influência da diagênese na redução da porosidade e permeabilidade criam grandes desafios para a exploração e produção desses reservatórios. O objetivo deste estudo é identificar os principais fatores deposicionais e diagenéticos que controlam a porosidade e permeabilidade dos carbonatos albianos no poço 3-OGX-61-RJS, localizado na área de Tubarão Azul, sul da Bacia de Campos, por meio de uma análise integrada faciológica, petrológica e petrofísica. As litofácies observadas incluem calcarenitos oolíticos, oncolíticos e peloidais, calciruditos oncolíticos e peloidais e arenitos híbridos, depositados em uma rampa carbonática rasa. As fácies deposicionais foram agrupadas em duas associações de fácies: uma rampa de carbonato proximal de alta energia composta por arenitos híbridos, calcarenitos oncolíticos e oolíticos e calciruditos oncolíticos, e uma rampa de carbonato intermediária de energia moderada composta por calcarenitos peloidais e oncolíticos com pelóides. As fácies deposicionais foram agrupadas em duas associações de fácies: uma rampa carbonática proximal de alta energia composta por arenitos híbridos, calcarenitos oncolíticos e oolíticos e calciruditos oncolíticos, e uma rampa de carbonática intermediária de moderada energia composta por calcarenitos peloidais e oncolíticos com pelóides. Nove petrofácies de reservatório foram definidas com base nos principais aspectos primários e diagenéticos de impacto na porosidade e permeabilidade. As rochas carbonáticas analisadas incluem calcarenitos oolíticos, oncolíticos, e peloidais, calcirruditos oncolíticos e peloidais e arenitos híbridos, depositados em uma rampa carbonática rasa. Nove petrofácies de reservatórios foram definidas com base nos principais aspectos texturais e composicionais primários e diagenéticos de impacto sobre a porosidade e a permeabilidade. Os principais processos diagenéticos observados foram a cimentação por calcita, a substituição por dolomita blocosa e pirita, a precipitação de caulinita, a compactação mecânica e química, incluindo estilolitização, e a dissolução eodiagenética e mesodiagenética. A textura e composição primária tiveram relativamente pouco impacto na qualidade dos reservatórios. A cimentação precoce parcial por franjas de calcita e crescimentos sintaxiais ajudou a preservar a porosidade primária dos calcarenitos oolíticos e oncolíticos dos efeitos da compactação. Onde a cimentação eodiagenética foi muito intensa, a porosidade interpartícula foi completamente obliterada. Arenitos hibridos com pouca ou nenhuma cimentação precoce tiveram sua porosidade e permeabilidade extremamente reduzida pelos efeitos da compactação. Estes processos fundamentais atuaram diretamente no controle da porosidade e permeabilidade das rochas estudadas.

Palavras-chave: Diagênese, Carbonatos, Petrografia.

1. Introduction

Campos Basin, offshore SE Brazil, is one of the most productive basins of the country, currently responsible for approximately 30% of oil and 20% of natural gas production (ANP, 2024). Carbonates of the Macaé Group constitute the reservoirs in large fields such as Pampo, Badejo, and Linguado (Bruhn *et al.*, 2003; Okubo *et al.*, 2015). These shallow-water marine carbonate reservoirs contain important oil accumulations in the center of the Campos Basin and are of great interest for both exploration and scientific research. These rocks have a diagenetic evolution with different levels of intensity of cementation, compaction, and dissolution processes that impacted the permeability and porosity of such important reservoirs (Carozzi *et al.*, 1983; Armelenti *et al.*, 2021). The objective of this work is to characterize the main depositional and diagenetic controls on reservoir quality in the Albian carbonate rocks of the Tubarão Azul Field area, located in the southern Campos Basin. To this end, an integrated study was developed, combining core sedimentology, systematic quantitative petrography, and petrophysical analyses. Defining the genetic conditions and distribution patterns of the processes that impacted the porosity and permeability of the shallow marine Albian carbonate rocks in the area will contribute to reducing exploration risks and optimizing the recovery of producing fields.

2. Study Area

2.1 Geological Settings

The Campos Basin is located at the eastern Brazilian margin, along the north coast of the Rio de Janeiro State and southern Espírito Santo State. It is separated from the Espírito Santo Basin to the north by the Vitória Arch, and from the Santos Basin to the south by the Cabo Frio Arch. The basin covers an area of approximately 115,000 km^2, with only a small onshore area of 5,800 km^2. The exploration well 3-OGX-61-RJS, the focus of the study, was drilled near Tubarão Azul Field in the southern portion of the Campos Basin (Fig. 1).

The Campos basin was formed during the Early Cretaceous as a consequence of the Gondwana breakup when the South American and African plates were separated by a rift system that propagated from south to north. The breakup led to the formation of a series of rift basins with different timing and filling, culminating with crustal rupture and expansion of the ocean floor (Dias *et al.*, 1990; Winter *et al.*, 2007). The tectonic and stratigraphic evolution of the Campos Basin is subdivided into three supersequences: Rift, Post- Rift and Drift. The rift sequence was deposited during the mechanical subsidence phase and includes basalts of the Cabiúnas Formation and continental sediments of the Lagoa Feia Formation. (Guardado *et al.*, 1988; Winter *et al.*, 2007). The post-rift sequence is characterized by the evaporites of the Retiro Formation deposited by marine transgression during relative tectonic quiescence (Dias *et al.*, 1990; Azevedo *et al.*, 2004). The drift phase consists of a marine sequence deposited under thermal subsidence affected by intense halokinesis. This stage begins with carbonate sedimentation of the Macaé Group, grading upwards to a mainly siliciclastic succession of the Campos Group (Winter *et al.*, 2007). Sedimentation within the Macaé Group occurred during Albian-Cenomanian in early drift context and comprises the Goitacás, Quissamã, Outeiro, Imbetiba, and Namorado formations. The Macaé Group consists of a thick carbonate section deposited in a transgressive marine context, representing the beginning of the drift phase of the Campos Basin (Winter *et al.*, 2007, Fig. 3). The Quissamã Formation (Fig. 2) has an average thickness of 800 m distributed along a NE trend (Spadini *et al.*, 1988), formed in a shallow neritic environment with a homoclinal carbonate ramp morphology (Guardado *et al.*, 1989; Carvalho *et al.*, 2002). The upper portion of the Quissamã Formation is formed by calcarenites and calcirudites (sense Grabau, 1904; Bramkamp & Powers, 1958) composed of oncoids, ooids, peloids, intraclasts, and bioclasts, stacked in shoaling-upward cycles up to 15 meters thick, interpreted as carbonate shoals deposited under shallow paleobathymetric conditions (Falkenhein *et al.*, 1981; Spadini 1992; Okubo *et al.*,2015).

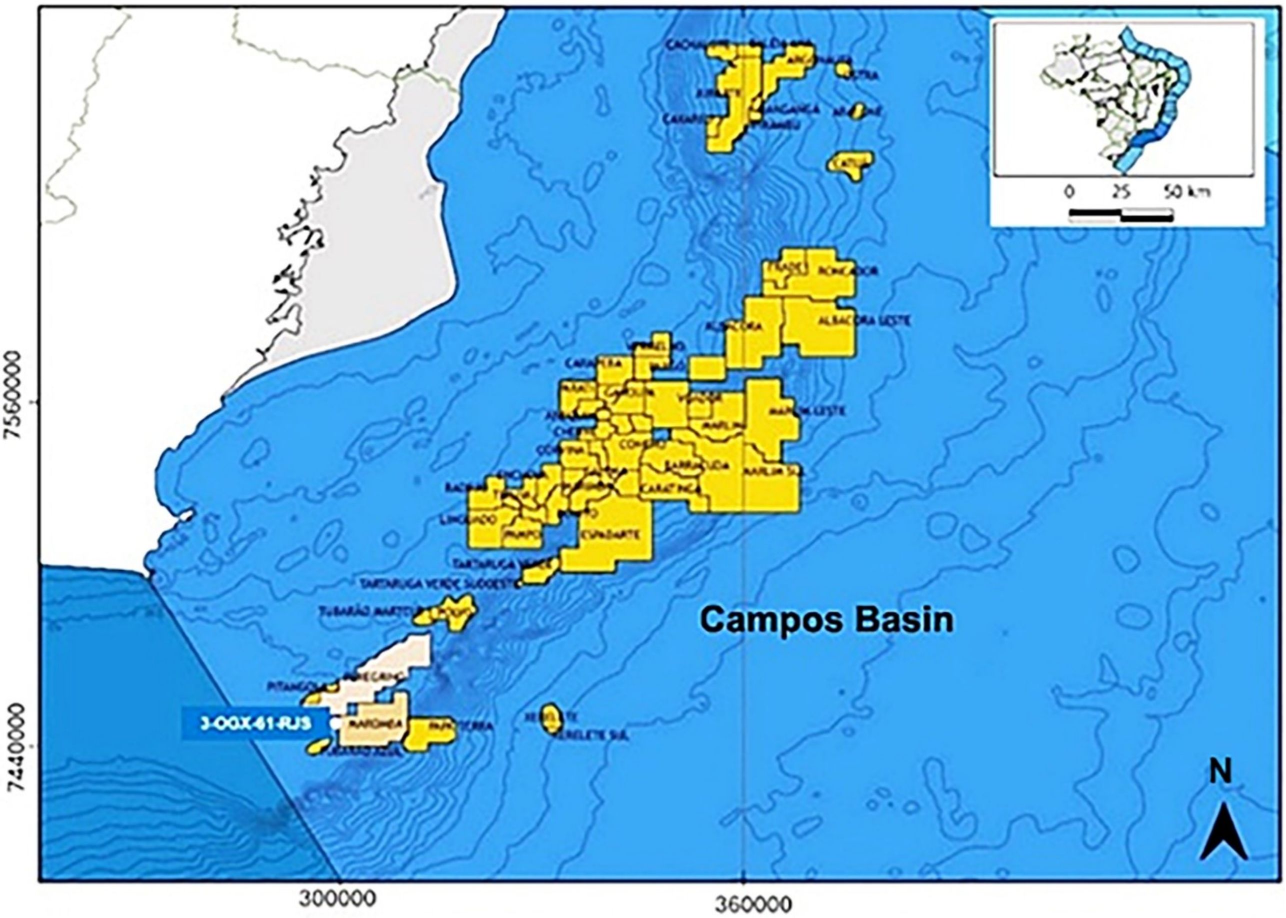

Figure 1. Location map of the study area where well 3-OGX-61-RJS is located in the Tubarão Azul field in the south of the Campos Basin.

Figura 1. Mapa de localização da área de estudo onde está localizado o poço 3-OGX-61-RJS no campo de Tubarão Azul no sul da Bacia de Campos.

The sediments of the Quissamã Formation were deposited in a hypersaline marine environment with restricted circulation. Carbon and oxygen isotopic data with values of +4‰ $\delta^{13}C$ and -2‰ $\delta^{18}O$ corroborate the interpretation of a hypersaline environment (Spadini *et al.*, 1988; Robaina *et al.*, 1993). Salt tectonics played an important role in the sedimentation of the Quissamã Formation (Amarante *et al.*, 2021). The highs on which shallow carbonate shoals with high-energy facies were deposited were generated through halokinesis (Figueiredo & Mohriak; 1984; Spadini *et al.*, 1988; Favoretto *et al.*, 2016). Some modern carbonate systems, such as the Grand Bahamas Bank, are considered depositional analogues to the Quissamã Formation carbonates, especially in terms of the geometry of the shallow carbonate banks (Okubo *et al.*, 2015).

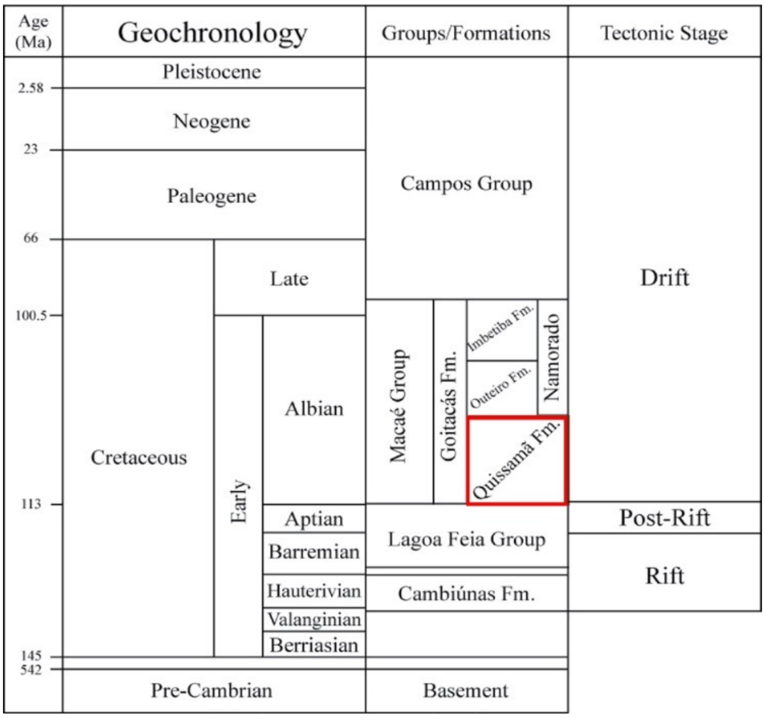

Figure 2. Tectono-stratigraphic chart of Campos Basin.

Figura 2. Carta estratigráfica da Bacia de Campos.

3. Materials and Methods

A sedimentological analysis was performed through a detailed core description of the 3-OGX-61-RJS well, where a 36.11 m thick succession was measured and represented in a sedimentological log at a 1:50 scale. The description of the textural aspects and the faciological interpretation of the core were supported by the petrographic characterization of the analyzed thin sections. Petrographic modal analysis was performed in 50 thin sections prepared from impregnated samples with blue epoxy resin. The thin sections were stained with a solution of alizarine red S and potassium ferrocyanide to identify the carbonate minerals (Dickson, 1965). The thin sections were systematically analyzed using polarized petrographic microscopes and the Petroledge® software (De Ros *et al.*, 2007). Quantification was performed by counting 300 points per thin section, following transects perpendicular to the lamination or grain orientation. Quantitative petrography aimed at the systematic characterization of the types, textural aspects, habits, locations, and paragenetic relations of primary and diagenetic constituents and pore types. The samples were classified using the nomenclature created by Grabau (1904) and modified by Bramkamp & Powers (1958). Reservoir petrofacies were defined using the concept proposed by De Ros & Goldberg (2007), aiming to evaluate the primary and diagenetic parameters that control and most impact the porosity and permeability of the studied samples. Digital photos of the main textural, primary, and diagenetic compositional features and the porosity of the slides were acquired using a Zeiss Axio petrographic microscope. A2 imager with an Axio camera. Furthermore, the thin sections were scanned and digitalized on Zeiss Axio equipment Scan Z1 with the Zen Blue 3.1 software at Solintec company. A log-based mineralogical petrophysical model was applied to 3-OGX-61-RJS well to obtain the main mineralogical constituents. The model was created using the Lithology Computation workflow from Techlog Software®, calibrated with the petrographic descriptions from the core. The mineralogical log was calculated for the percentage of calcite, dolomite, silica, and clay, based on gamma ray, density, neutron, resistivity, sonic profiles, and basic petrophysical analyses. Available conventional petrophysical porosity and permeability analyses were integrated with the petrographic data and observations to recognize patterns, calculate microporosity, and calibrate the log analysis.

4. Results

4.1 Petrography of the Quissamã Formation

Carbonate rocks analyzed in well 3-OGX-61-RJS comprise calcarenites and calcirudites (sense Grabau 1904; Bramkamp & Powers, 1958), with few hybrid arenites (Zuffa 1980). The calcarenites are predominantly massive and fractured and rarely have plane-parallel lamination with stylolites. The calcirudites are predominantly massive, compacted, and stylolitized. The main allochemical particles in calcarenites are oncoids, ooids, peloids, microbial, and particulate carbonate intraclasts, bioclasts of bivalves, echinoids, red algae, benthic and planktic foraminifera, ostracods and rare gastropods and bryozoans. Other primary constituents are phosphatic bioclasts, sub-angular grains of quartz, feldspars, biotite, and glauconite peloids (Table 1). Ooids vary in size from fine to coarse sand, some with a radial structure (Fig. 3A). Many are micritized, and some are polycomposite, consisting of two or more grouped ooids (Fig. 3B), up to very coarse sand in grain size. The oncoids are irregular, ranging from medium to very coarse sand, and are partially micritized. Agglomerate oncoids are common, with nuclei of siliciclastic grains and bioclasts. Peloids are abundant and range in size from fine sand to coarse sand, predominantly fine sand. (Fig. 3C).

Calcirudites are highly compacted, and many samples show stylolites due to intense chemical compaction (Fig. 3D and E). Particulate carbonate intraclasts are common, ranging in size from coarse sand to pebble. Microbial intraclasts range from medium sand to pebble, with a clotted texture are rare. The diversity and volume of bioclasts is relatively low in the rocks studied (Table 2). The most common bioclasts are disarticulated bivalves, often fractured, some strongly micritized, commonly recrystallized or dissolved, and filled with mosaic drusiform calcite. Echinoid bioclasts commonly show syntaxial overgrowths. Gastropod bioclasts are typically micritized or dissolved and filled with mosaic calcite or, more rarely, blocky dolomite. Planktic foraminifera and red algal bioclasts are rare and usually partially micritized.

The hybrid arenites (Fig. 3F) occur intercalated with the carbonate rocks. They are predominantly massive and well-selected. The siliciclastic grains are angular to subangular and range from fine to coarse sand, with a predominantly fine sand size. The dominant primary constituents are monocrystalline quartz, feldspars (microcline, orthoclase, and plagioclase), muscovite, biotite, ooids, bioclasts, and rare phosphatic bioclasts (Table 3).

Table 1. Main primary constituents of the Quissamã Calcarenites.

Tabela 1. Principais constituintes primários dos Calcarenitos da Formação Quissamã.

Main primary constituents	Average %	Maximum %
Ooids	11	30
Oncoids	22	37
Peloids	25	54
Carbonate bioclasts	2	8
Peloidal matrix	<1	6
Microbial intraclasts	<1	3.5
Particulate carbonate intraclasts	2.3	8
Phosphatic bioclasts	<1	2.5
Monocrystalline quartz	<1	2.3
Microcline	<1	6

Table 2. Main primary constituents of the Quissamã Calcirudites.

Tabela 2. Principais constituintes primários dos Calcirruditos da Formação Quissamã.

Main primary constituents	Average %	Maximum %
Ooids	9.6	24.9
Oncoids	25	35
Peloids	16	40
Carbonate bioclasts	4.5	11
Peloidal matrix	<1	4.5
Microbial intraclasts	<1	4
Particulate carbonate intraclasts	2.5	8
Phosphatic bioclasts	<1	1.5
Monocrystalline quartz	<1	2.5
Microcline	<1	5.2

Table 3. Main primary constituents of the Quissamã Hybrid arenites.

Tabela 3. Principais constituintes primários dos Arenitos Híbridos da Formação Quissamã.

Main primary constituents	Average %	Maximum %
Monocrystalline quartz	22.56	25
Microcline	8.24	10.33
Orthoclase	1.33	2
Plagioclase	2.11	2.33
Muscovite	1.44	2.33
Biotite	1.33	2
Carbonate peloides	2.44	4
Carbonate bioclasts	1	5.33
Phosphatic bioclasts	<1	<1
Ooids	2.11	3
Oncoids	1.33	2

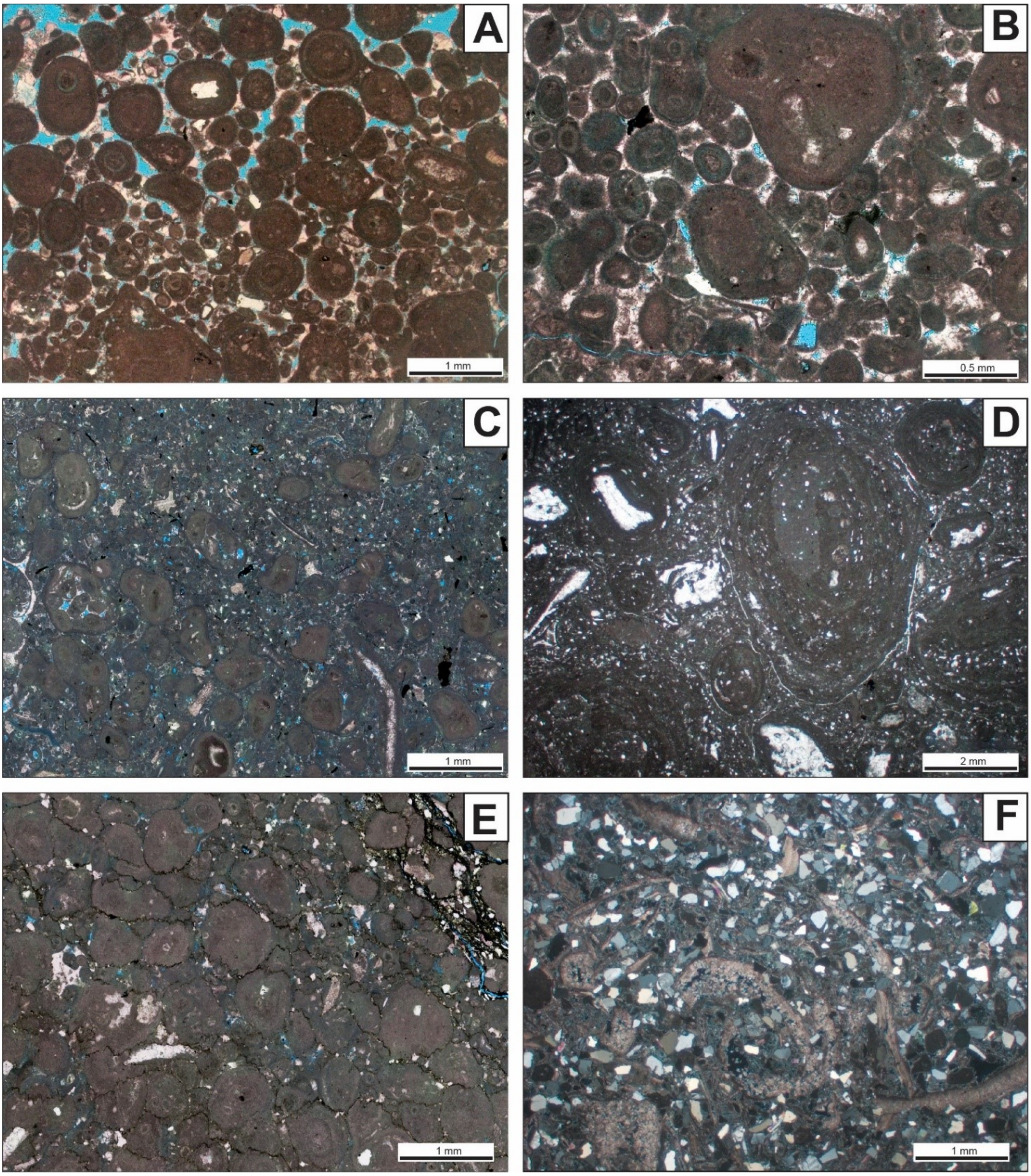

Figure 3. Main lithological types and primary constituents of the studied Quissamã Formation rocks: A) Oolitic calcarenite with partially preserved primary porosity. Uncrossed polarizers (//P). B) Oolitic calcarenite with polycomposite ooids. //P. C) Oncolitic-peloidal calcarenite composed of oncoids, peloids and bioclasts. //P. D) Oncolitic calcirudite composed of oncoids and peloids. Crossed polarizers (XP). E) Calcirudite is composed of oncoids and peloids with intense compaction and stylolites. //P, F) Hybrid sandstone comprises quartz grains, feldspars and bivalve bioclasts. XP.

Figura 3. Principais tipos litológicos e constituintes primários característicos das rochas carbonáticas da formação Quissamã: A) Calcarenito oolítico com porosidade primária preservada. Polarizadores descruzados (//P). B) Calcarenito oolítico com oolitos policompostos. //P. C) Calcarenito oncolítico composto por oncolitos, pelóides e bioclastos. //P. D) Calcirrudito oncolítico composto por oncolitos e pelóides. Polarizadores cruzados (XP). E) Calcirrudito composto por oncolitos e pelóides com intensa compactação e estilolitos. //P, F) Arenito híbrido composto por grãos de quartzo, feldspatos e bioclastos de bivalves. XP.

The main diagenetic constituents in the calcarenites are: calcite, dolomite, pyrite, kaolinite, and traces of sulfate such as gypsum and anhydrite. (Table 4). Calcite is the main diagenetic constituent and occurs in the form of rims (Fig. 4 A), syntaxial overgrowths on echinoid bioclasts (Fig. 4B), and mosaic (Fig. 4C and 4D) cementing interparticle and intraparticle pores in ooids, oncoids and bioclasts, and as blocky crystals filling interparticle and fracture pores. Poikilotopic calcite is rare and occurs locally, filling interparticle pores. Dolomite occurs in lower volumes, in the form of small blocky crystals filling intraparticle pores in ooids (Fig. 4E), oncoids, and bioclasts of gastropods and bivalves, saddle dolomite is rare and commonly fills interparticle pores (Fig. 4F). Framboidal and microcrystalline pyrite is common, replacing ooids, oncoids, peloids, bioclasts, and biotite. The main diagenetic constituents in the calcirudites are: calcite, dolomite, pyrite, and kaolinite. Similarly to calcarenites, the most abundant constituent observed in calcirudites is calcite in the form of fringes covering the particles and in mosaic cementing interparticle and intraparticle pores. Dolomite occurs in much smaller volumes in the form of blocky crystals filling interparticle and intraparticle pores. Microcrystalline pyrite commonly replaces ooids, oncoids, and mainly biotite (Table 5).

The main diagenetic constituents observed in hybrid arenites are calcite rims, mosaic calcite filling intergranular pores, and intraparticle calcite in bivalve bioclasts. Kaolinite occurs as booklets replacing feldspars and lamellar expanding muscovite, and overgrowths of quartz and k-feldspar occur on some grains. Microcrystalline pyrite occurs replacing biotite (Table 6). Compaction was an important factor in permeability and porosity reduction in these rocks. Some feldspars and bioclasts are fractured. Rocks with a coarser texture have normal packing, and some primary interparticle porosity is preserved, while the finer are very compacted. Minor primary intergranular porosity is preserved in a few of the hybrid arenites, while secondary porosity is significant, with the dissolution of grains of feldspars, ooids, and bioclasts generating intragranular, intraparticle, and moldic pores.

Table 4. Main diagenetic constituents of the Quissamã Calcarenites.

Tabela 4. Principais consitutintes diagenéticos dos Calcarenitos da Formação Quissamã.

Main diagenetic constituents	Average %	Maximum %
Total Calcite	15.7	30.33
Interparticle calcite	13.4	29
Intraparticle calcite	2	5.3
Calcite filling fracture pores	<1	3.3
Total Dolomite	4.5	14
Interparticle dolomite	1.5	10
Intraparticle dolomite	2.33	12
Total Pyrite	2.5	4.5
Intraparticle replacement pyrite	<1	3
Intraparticle pore filling pyrite	<1	2.5

Table 5. Main diagenetic constituents of the Quissamã Calcirudites.

Tabela 5. Principais constituintes diagenéticos dos Calcirruditos da Formação Quissamã.

Main diagenetic constituents	Average %	Maximum %
Total Calcite	18.11	25.8
Interparticle calcite	10.58	24
Intraparticle calcite	3.5	6
Calcite filling fracture pores	<1	2.33
Total Dolomite	3.57	9
Interparticle dolomite	2.14	8
Intraparticle dolomite	1.7	5
Total Pyrite	4.21	6
Intraparticle replacement pyrite	<1	2.33
Intraparticle pore filling pyrite	<1	3

Table 6. Main diagenetic constituents of the Quissamã Hybrid arenites.

Tabela 6. Principais consitutintes diagenéticos dos Arenitos Híbridos da Formação Quissamã.

Main diagenetic constituents	Average %	Maximum %
Total Calcite	22.67	30.66
Interparticle calcite	12.44	15.66
Intraparticle calcite	10.22	15
Calcite filling fracture pores	<1	<1
Total Dolomite	1.34	2
Interparticle dolomite	0.89	1.33
Intraparticle dolomite	<1	<1
Total Kaolinite	4.99	6,33
Total Pyrite	3.67	5
Intraparticle replacement pyrite	<1	4.33
Intraparticle pore filling pyrite	<1	1.5
K-Feldspar Overgrowth	2.67	4.33
Quartz Overgrowth	1.56	2.67

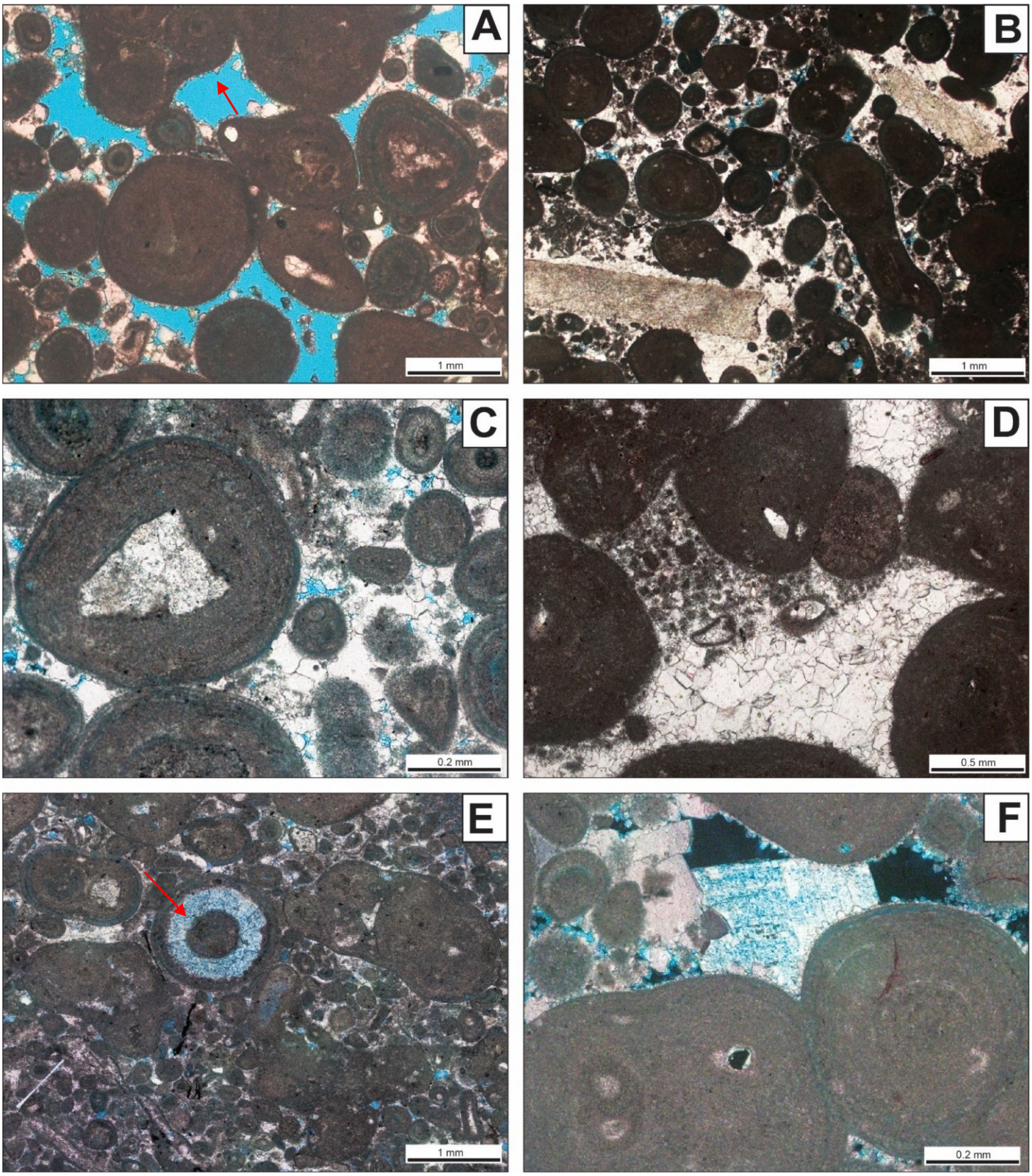

Figure 4: Characteristic diagenetic constituents of carbonate rocks of the Quissamã Formation: A) Calcite rims covering particles. (red arrow) //P. B) Syntaxial calcite around echinoid bioclasts. //P. C) Calcarenite cemented by mosaic calcite filling the intraparticle and interparticle pores. //P. D) Calcarenite with oncoids cemented by calcite in a drusiform mosaic. //P. E) Ferroan blocky dolomite (stained blue) filling intraparticle pore in ooid (red arrow). //P F) Saddle dolomite filling partially interparticle pore. XP.

Figura 4. Constituintes diagenéticos característicos das rochas carbonáticas da formação Quissamã: A) Franjas de calcita cobrindo as partículas em calcarenito oolítico. (seta vermelha) //P. B) Crescimentos sintaxiais de calcita em torno de bioclastos de equinóides, //P. C) Calcarenito oncolítico cimentado por calcita em mosaico nos poros intrapartícula e interpartícula. //P. D) Calcarenito oncolítico cimentado por calcita em mosaico drusiforme. //P. E) Cristais de dolomita blocosa ferrosa em poro intrapartícula em oolito (seta vermelha). //P F) Dolomita em sela preenchendo poro interpartícula. XP.

Most of the porosity in the analyzed samples corresponds to fabric-selective types sensu Choquette & Pray (1970), and less commonly to non-fabric-selective types (Table 7 & 8). Primary interparticle porosity is predominant in ooids calcarenites (Fig.5 A) and, due to limited cementation and compaction of some samples. Compaction is very intense in fine-grained peloidal calcarenites. Most of these samples have extremely low primary interparticle porosity and permeability. Secondary intraparticle porosity occurs mainly within dissolved oncoids and ooids (Fig. 5B and 5E). Part of these pores was generated by the dissolution of feldspar grains that constituted the nuclei of these particles and, to a lesser extent, of bivalve and gastropod bioclasts. Moldic pores are more common in coarse calcarenites. Vugular pores are more common in calcarenites with oncoids (Fig. 5C) but in smaller volumes than other pore types. In hybrid arenites, most of the porosity is secondary, generated by the dissolution of feldspars (Fig. 5D), oncoids, and bioclasts. Micropores less than 10 μm in size occur mainly in peloids, ooids, and oncoids. Fracture (Fig. 5F) and channel pores generated by dissolution along stylolites are rarer, occurring locally in some samples.

Most of the porosity observed in hybrid arenites is derived from the dissolution of feldspar grains and moldic pores. Intergranular porosity is low, and fracture pores are rare. (Table 9). The pore system of the carbonate rocks from the Quissamã Formation in 3-OGX-61-RJS well is complex, with preservation of primary interparticle porosity in some samples, while others are very compacted and cemented, without preservation of primary porosity. Microporosity, calculated by subtracting the petrographic porosity from the petrophysical porosity, is, on average, 8.35%, with a maximum value of 18%. Petrophysical porosity is, on average, 11.4%, with a maximum value of 19%. Horizontal permeability averages 3.12 mD, with a maximum value of 35.4 mD.

Table 7. Main types of pores observed Quissamã Calcarenites.

Tabela 7. Principais tipos de poros observados nos Calcarenitos da Formação Quissamã.

Types of pores	Average %	Maximum %
Primary interparticle	4.57	14
Secondary intraparticle	4.85	6.67
Moldic	<1	3
Vugular	<1	2.33
Channel	<1	0.67
Rock fracture	<1	1.33
Grain fracture	<1	<1
Intragranular in feldspars	<1	<1

Table 8. Main types of pores observed Quissamã Calcirudites.

Tabela 8. Principais tipos de poros observados nos Calcirruditos da Formação Quissamã.

Types of pores	Average %	Maximum %
Primary interparticle	3.67	9.67
Secondary intraparticle	6	12.67
Moldic	<1	1.33
Vugular	<1	2.67
Channel	<1	<1
Rock fracture	<1	1.67
Grain fracture	<1	<1
Intragranular in feldspars	<1	<1

Table 9. Main types of pores observed Quissamã Hybrid arenites.

Tabela 9. Principais tipos de poros observados nos Arenitos Híbridos da Formação Quissamã.

Types of pores	Average %	Maximum %
Primary intergranular	6.67	9
Intragranular in feldspars	9.21	11
Moldic	2.67	4.5
Vugular	<1	1.67
Channel	<1	<1
Rock fracture	<1	<1
Grain fracture	<1	<1

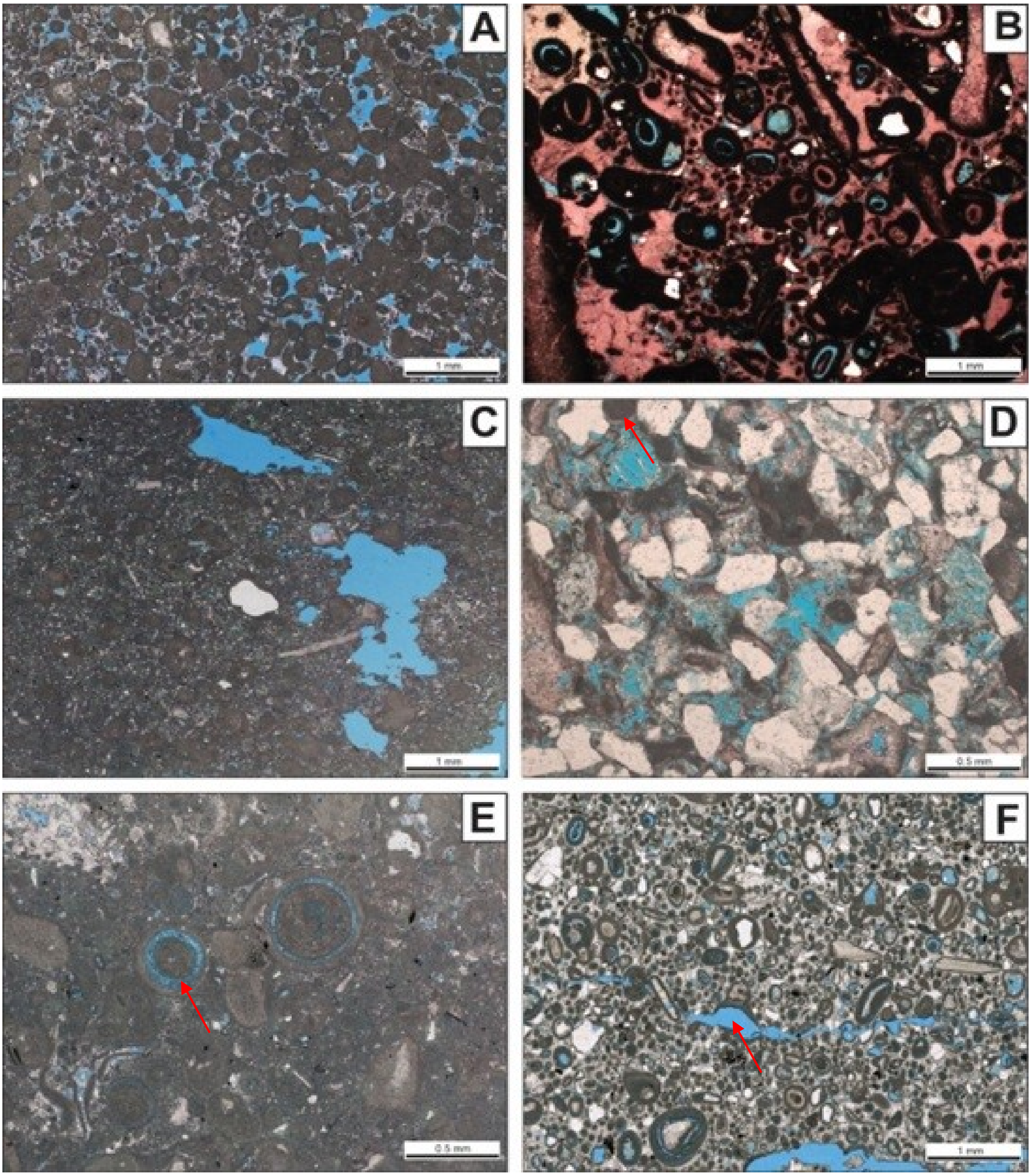

Figure 5. Porosity aspects of the analyzed samples: A) Primary interparticle porosity. //P. B) Intraparticle porosity in ooids and oncoids. Macrocrystalline calcite cement-stained pink. XP. C) Vuggy pores. //P. D) Intragranular and moldic porosity in hybrid arenite (red arrow). //P. E) Envelops partially dissolved, intraparticle pores in ooids. (red arrow) //P. F) Fracture and intraparticle porosity. (red arrow) //P.

Figura 5. Aspectos da porosidade das amostras analisadas: A) Porosidade interpartícula primária. //P. B) Porosidade intrapartícula em oolitos e oncolitos. XP C) Porosidade vugular; //P. D) Porosidade intragranular e móldica em arenito híbrido. //P. E) Envelopes parcialmente disssolvidos em oolitos. (seta vermelha) //P. F) Porosidade de fratura (seta vermelha) e intrapartícula.

4.2 Depositional Facies of the Quissamã Formation

A total of 36.19 m of core from the Quissamã Formation were described in 3-OGX-61-RJS well, on a 1:50 scale, with description supported by the petrographic analyses. Six depositional facies were recognized in the studied samples (Table 10; Figure 6). The facies were grouped into two facies associations: High-energy shallow carbonate ramp (HYR, OOCA, OCR, PCR) and Moderate-energy intermediate carbonate ramp (PELC, OCA).

Table 10. Lithofacies of the Quissamã Formation in the analyzed well 3-OGX-61-RJS (Figure 6).

Tabela 10. Tabela de fácies da seção estudada no poço 3-OGX-61-RJS (Figura 6).

Facies	Facies Description	Facies Association
PELC	Peloidal calcarenites, with oncoids and rare bioclasts of bivalves and echinoids. Containing some quartz grains, feldspars and biotite. Dominantly massive, with the local occurrence of horizontal lamination. Locally fractured, with stylolites and dissolution seams. (Fig. 7A).	Moderate energy, deeper portions of carbonate shoals
OCA	Oncolitic calcarenites, with variable proportions of peloids and bioclasts of bivalves, echinoids, and gastropods. It may contain grains of quartz, feldspars, and biotite. Dominantly massive, locally with high or low angle cross-stratification. Locally fractured, with stylolites and dissolution seams. (Figure. 7B).	
HYAR	Hybrid arenites comprise siliciclastic grains (quartz, feldspars, micas) and carbonate particles (ooids, oncoids, bioclasts, and peloids). Rarely with mud lenses. Massive or commonly with high-angle or low-angle cross-bedding and truncated wavy lamination. Locally dolomitized, bioturbated, fluidized and fractured. Stylolites may occur. Saturated with oil. (Fig. 7C).	High energy, shallower portions of carbonate shoals, under wave- and current-action
OOCA	Oolitic calcarenites with variable proportions of oncoids, peloids and rare bivalve and echinoid bioclasts. It may contain grains of quartz, feldspars, and micas. Dominantly massive, with an occurrence of low-angle cross-stratification. Locally fractured, with stylolites and dissolution seams. Locally bioturbated. (Fig.7D).	
OCR	Oncolitic calcirudites with intraclasts, peloids, and bioclasts (echinoids, bivalves, and gastropods). It may contain grains of quartz, feldspars, and micas. Dominantly massive, with an occurrence of high-angle cross-stratification. Locally fractured, with stylolites and dissolution seams. Bioturbation and local fluidization and dolomitization. (Fig. 6 E)	
PCR	Peloidal calcirudites, with oncoids and rare bioclasts (bivalves and echinoids). Locally stylolitized and bioturbated. (Fig. 7F)	

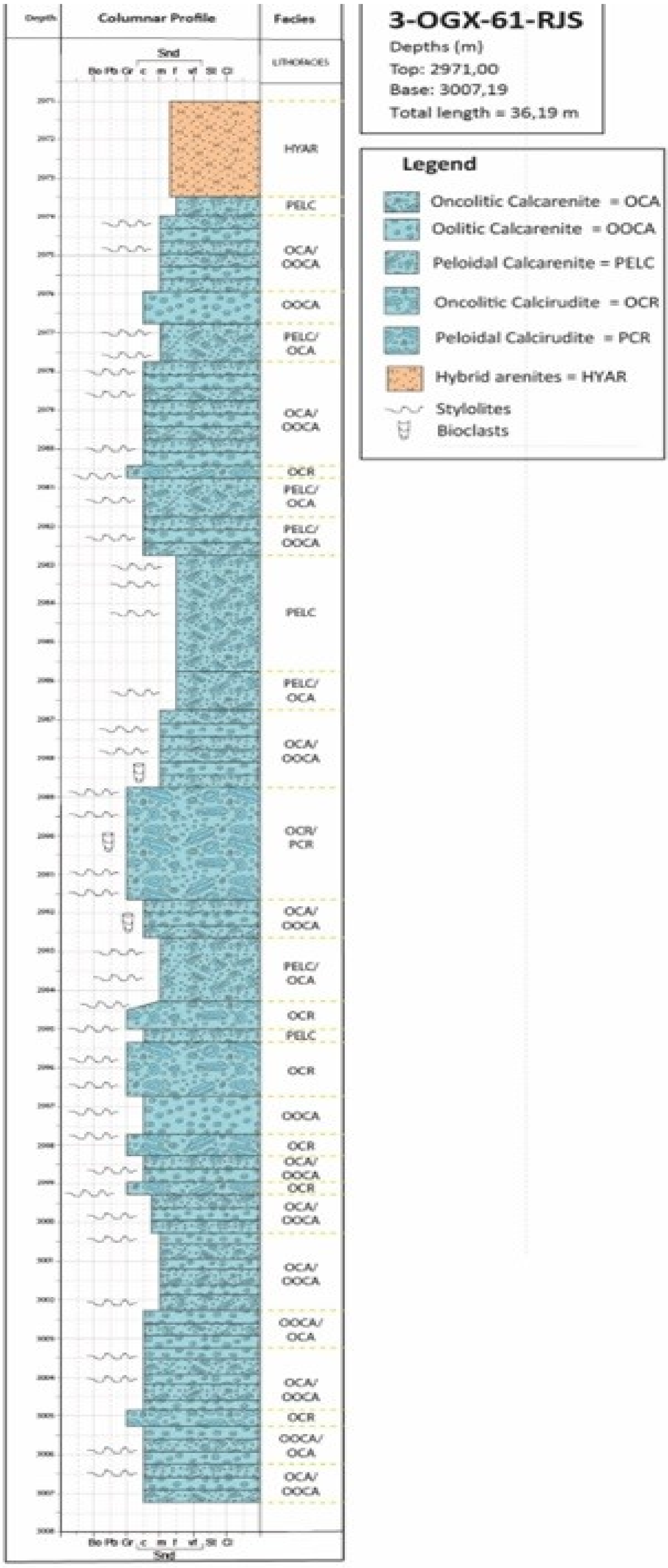

Figure 6. The lithological log of the core was analyzed in the 3-OGX-61-RJS well.

Figura 6. Perfil litológico colunar do testemunho analisado no poço 3-OGX-61-RJS.

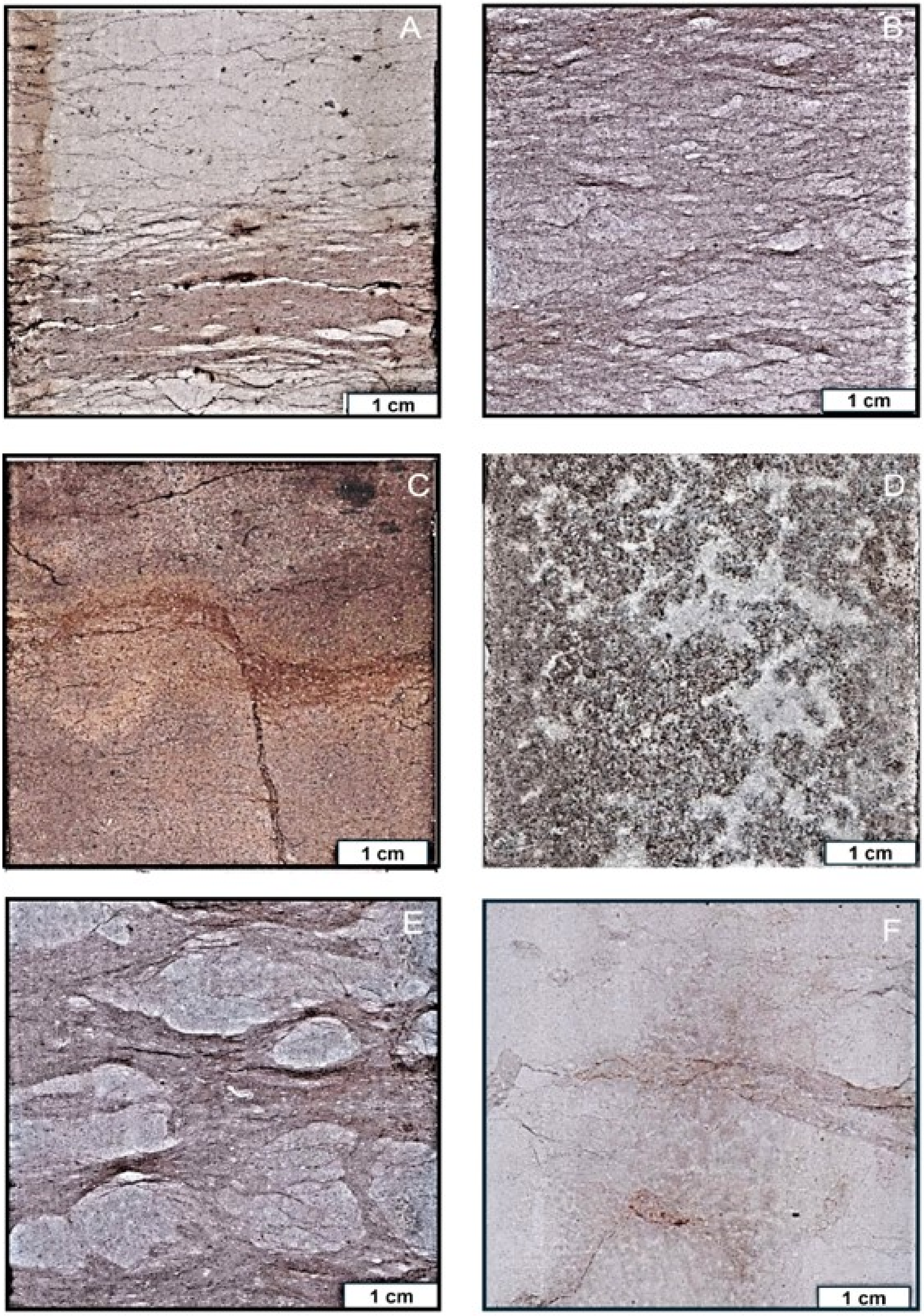

Figure 7. Main facies analyzed in 3-OGX-61-RJS well: A) Peloidal calcarenite (PELC) with stylolites. B) Oncolitic calcarenite (OCA). C) Hybrid arenite (HYAR) saturated with oil. D) Oolitic calcarenite (OOCA), E) Oncolitic calcirudite (OCR). F) Peloidal calcirudite (PCR).

Figura 7. Principais fácies analisadas no poço 3-OGX-61-RJS: A) Calcarenito peloidal (PELC) com estilolitos. B) Calcarenito oncolítico (OCA). C) Arenito híbrido (HYAR) saturado com óleo. D) Calcarenito oolítico (OOCA), E) Calcirrudito oncolítico (OCR). F) Calcirrudito peloidal (PCR).

5. Discussion

5.1 Depositional Environment of the Quissamã Formation

The depositional environment of the Macaé Group corresponds to an extensive homoclinal carbonate ramp (Spadini *et al.*, 1988) deposited along a NE-trending belt. The basal portion of the Quissamã Formation is characterized by shallow carbonate deposits, characteristically dolomitized (Búzios Member). The compositional and textural variety of carbonate sediments is essentially related to the depth variation within the ramp (Spadini 1992; Carvalho *et al.*, 2002; Okubo *et al.*, 2015).

The Albian carbonate reservoirs correspond elongated shoals, NE-oriented, approximately 20 m thick, <1 km wide, and up to 2.5 km long, and are composed mainly of calcarenites constituted by oncoids, peloids, ooids, and rare bioclasts (Bruhn, *et al.*, 2003). These shoals are considered small analogues of the elongated Joulter Cays bodies and the Exumas Islands in the Bahamas, with average shore lengths varying between 30 and 45 km long and 10 to 15 km wide (Okubo *et al.*, 2015). Depositional models of carbonate sediments from Lily Bank (Bahamas) reveal micrite-free sediments at shoal crests, while finer sediments are deposited in relatively lower-energy interbank depressions (Rankey *et al.*,2006). This configuration suggests a direct relationship between bathymetry, hydrodynamic energy, and particle size found in the different physiographic positions of the shoals.

Previous studies have defined different facies in the Quissamã Formation, relating textures, fabric, and selection to the energy of the depositional environment (Spadini *et al.*, 1988; Guardado *et al.*, 1989). In our work, two facies associations were recognized. The first is composed of peloidal and oncolitic calcarenites and calcirudites deposited in moderate energy settings, on the flank of shoals, i.e., zones that were protected from most of the action of waves and currents. The second facies association is composed of oolitic and oncolitic calcarenites and calcirudites and hybrid carbonate-siliciclastic arenites deposited in high-energy settings, corresponding to the crest of the shoals, directly impacted by the action of waves and currents. These facies associations occur interspersed throughout the studied interval, highlighting changes in the relative base-level and, therefore, shifts in the relative position of the carbonate shoals, resulting in the alternation of energy in the paleoenvironment. The depositional environment was an important factor in defining the volume of primary porosity in the studied carbonate rocks, but the main mechanism controlling the reservoir quality of the studied rocks was the intensity of diagenetic processes.

5.2 Diagenetic Evolution of the Quissamã Formation

The sequence of observed diagenetic processes and products that affected the rocks studied in the well of the Quissamã Formation was interpreted based on the distribution of diagenetic constituents and their paragenetic relationships with the primary constituents, other diagenetic constituents, and with the porosity (Figure 8). The paragenetic sequence observed in this study can be summarized as:

1) Intense or partial micritization of allochemical particles.

2) Framboidal and microcrystalline pyrite replacing the allochemical particles and biotite.

3) Fibrous rims of aragonite or magnesian calcite covering the allochemical particles.

4) Syntaxial calcite overgrowths on echinoid bioclasts.

5) Dissolution of allochemical particles and feldspars. Generation of intraparticle and intragranular porosity.

6) Autigenesis of kaolinite replacing feldspars, expanding and replacing muscovite, and filling intraparticle and moldic pores.

7) Blocky dolomite locally filling intraparticle and moldic pores, and replacing calcite cement and allochemical particles.

8) Mechanical compaction, evidenced by the rearrangement of grains and local fracturing of bioclasts.

9) Recrystallization of fibrous carbonate rims.

10) Intense cementation by mosaic calcite.

11) Chemical compaction, generating sutured interparticle contacts and stylolites.

12) Dissolution along stylolites, formation of channel and vugular pores, intraparticle dissolution of ooids and oncoids.

13) Limited precipitation of saddle dolomite.

14) Mosaic calcite precipitation in pores partially replacing dolomite

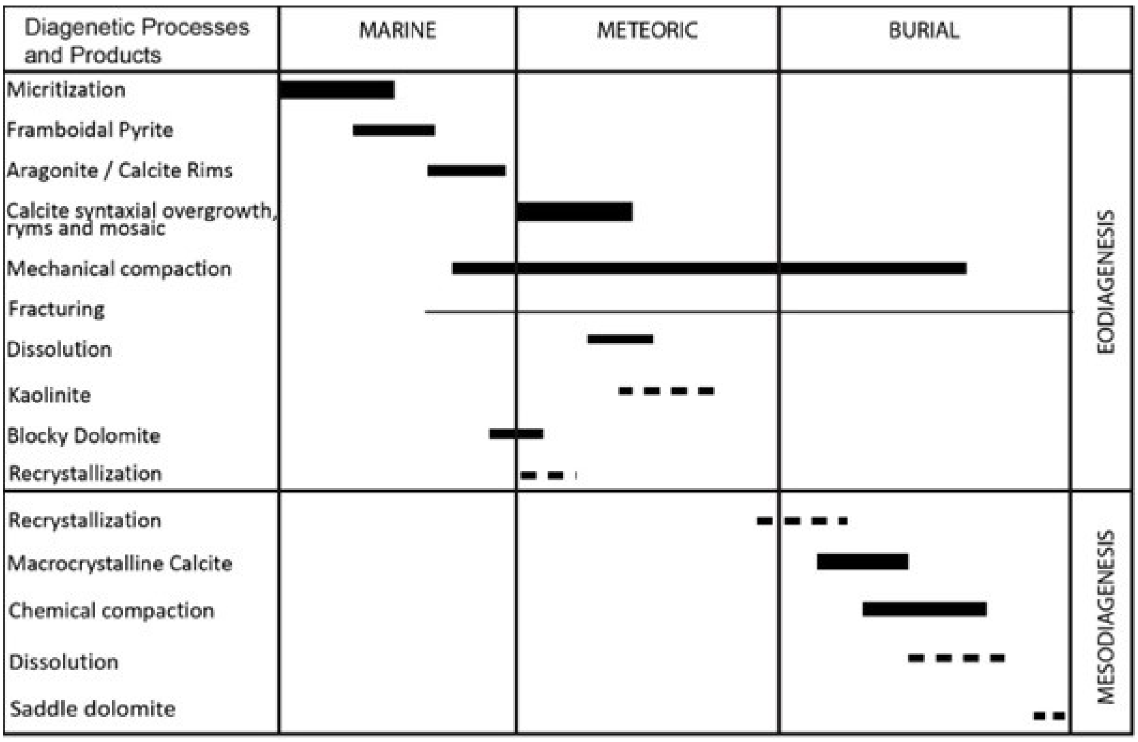

Figure 8. The schematic diagenetic sequence of the analyzed samples from the Quissamã Formation. The thickness of the bars represents the intensity of each process.

Figura 8. Sequência diagenética esquemática das amostras analisadas da Formação Quissamã. A espessura das barras representa a intensidade de cada processo.

The intense micritization observed in allochemical particles, mainly in ooids and oncoids, occurred in a stagnant phreatic marine environment under the action of microorganisms (Longman, 1980; Tucker & Wright; 1990; Moore & Wade, 2013). Under these same conditions, microcrystalline and framboidal pyrite were precipitated by bacterial reduction of the sulfate from seawater (Berner, 1984), commonly replacing primary constituents, especially biotite. In the active marine phreatic zone, characterized by seawater circulation by currents and waves, fibrous and microcrystalline rims made originally of aragonite or magnesian calcite covered the allochemical particles (Longman, 1980). The recrystallization of the microcrystalline rims probably occurred in a stagnant meteoric phreatic environment (Longman, 1980; Moore & Wade, 2013). Under phreatic conditions of active circulation of meteoric water, there was precipitation of syntaxial calcite overgrowths around echinoid bioclasts, the development of prismatic rims around other particles and the precipitation of mosaic calcite filling interparticle and dissolution pores (Longman, 1980; Moore & Wade, 2013).

The generation of secondary porosity in the studied rocks is related to the percolation of meteoric waters, resulting from the episodic exposure of carbonate shoals. The partial or total dissolution of ooids, oncoids, peloids, and bioclasts generated intraparticle microporosity, and intraparticle, moldic and vugular pores in most of the samples. The dissolution of previously micritized allochemical particles was important in the evolution of oolitic and oncolitic calcarenites, in a similar way to what was observed by Morad *et al.* (2018) in oolitic grainstones and packstones from the Arab D Formation (Late Jurassic). In an onshore gas field located southwest of Abu Dhabi, these authors observed that the micritization of allochemical particles promoted an increase in water-rock reactions, due to the greater surface area of the micritized particles. According to the authors, the dissolved carbonate is interpreted to have been redistributed as calcite cements in drusiform habits and syntaxial overgrowths (Morad *et al.*, 2018). Authigenic kaolinite was generated by the interaction of feldspars and micas with dilute meteoric waters (Worden & Morad, 2003), probably related to the periodic exposure of carbonate the shoals. The origin of the blocky dolomite crystals that replaced peloids, ooids, and calcite cements and rarely filled intraparticle dissolution pores in oncoids and ooids is probably related to the mixing of meteoric and marine fluids (Moore & Wade, 2013).

These small blocky dolomite crystals were residually concentrated throughout stylolites, as observed by Paganoni, *et al.* (2016), due to the lower solubility and greater resistance of dolomite to dissolution by pressure. Saddle dolomite precipitated mainly in secondary pores, under mesodiagenetic conditions, during burial (Spötl & Pitman, 1998; Machel, 2004). The progressive burial during mesodiagenesis promoted chemical compaction by pressure dissolution, forming sutured interparticle contacts and of stylolites. Late cementation by macrocrystalline calcite filled the interparticle, vugular, fracture and intraparticle pores, and replaced eodiagenetic cements such as kaolinite and dolomite. Some samples have secondary porosity generation through channel pores along stylolites and fractures, and as intraparticle dissolution pores. Some of this porosity formed by mesodiagenetic dissolution was filled by late dolomite, calcite, and pyrite. A second fracturing event occurred beneath deep burial. These fractures cut stylolites and compacted allochemical particles and were enlarged by dissolution to form channel pores.

5.3 Diagenetic controls on the porosity of the Quissamã Formation and analogues

Diagenesis promoted considerable complexity in the pore system of the analyzed Quissamã Formation samples, and petrographic evidence demonstrated that depositional texture and composition do not seem to have greatly influenced the quality of these reservoirs. Cementation and compaction intensely reduced the primary interparticle porosity of the rocks. The oolitic calcarenites deposited in high-energy environments on the top of the shoals, and the moderate-energy oncolitic calcarenites deposited along the flanks of the shoals have relatively good porosity and permeability. The preservation of primary interparticle porosity was essentially conditioned by limited early cementation. The rocks with good porosity and permeability are those with partial cementation by calcite rims covering the allochemical particles, and by syntaxial growths on echinoid bioclasts. Such limited early cementation supported the framework of these rocks, preventing the strong reduction of their interparticle porosity through compaction. High-energy oolitic deposits and moderate-energy oncolitic deposits can, therefore, present good or poor reservoir quality, depending more on the intensity of diagenetic processes than on depositional facies.

Compaction acted heterogeneously on the samples, with intensely compacted intervals interspersed with others with normal packing. The samples that suffered the greatest compaction are made up of fine to medium sand-sized peloids, with little or no eodiagenetic cementation. These samples had their porosity and permeability strongly reduced by intense compaction. Mosaic and macrocrystalline calcite cementation filled much of the interparticle porosity in most samples. Secondary intraparticle microporosity is more common in ooids than in oncoids, peloids and bioclasts. The average microporosity of the analyzed samples is 6.3% (Table 11). These micropores are poorly connected, which makes these ineffective for reservoir quality (Sellwood & Beckett, 1991). Part of the microporosity within the ooids was generated during mesodiagenesis, as these micropores are more abundant close to the and fractures and channel pores along the stylolites. Some alternatives for the fluids responsible for the secondary dissolution porosity generated in the Quissamã Formation during burial may be: CO_2 and organic acids generated by the diagenesis of organic matter in associated source rocks (Mazzulo & Harris, 1991), H2S from thermal sulfate reduction (Machel, 2001), or by processes of thermal imbalance of the fluid mixture within the reservoir (Giles & De Boer 1989).

Some oil fields have depositional and diagenetic histories similar to the studied Quissamã carbonates. One example is Waker Creek Field, located in southern Arkansas, United States. These reservoirs are Jurassic oolitic grainstones and packstones of the Smackover Formation, deposited in a marine shallow-water, high-energy environment (Blienfnick & Kaldi, 1996). In samples from the Waker Creek Field, analogous to those observed in this study, the porosity of facies dominated by peloids and oncoids without early marine cementation was completely destroyed by mechanical compaction (Blienfnick & Kaldi, 1996). With the progressive burial, chemical compaction became the main diagenetic process resulting in sutured interparticle contacts, further reducing porosity and permeability. After mechanical compaction and advanced-stage cementation related to chemical compaction, pore enlargement occurred through partial dissolution of particles and cement. Late-stage dissolution occurred along paths of preserved primary porosity (Blienfnick & Kaldi ,1996).

Another example of carbonate rocks with a diagenetic control similar to that observed in the Quissamã Formation occurs in the Humbly Grove Field located in the Weald Basin, Southern England, where the main oil reservoirs are ooidal grainstones and packstones, from the Middle Jurassic Great Oolite Formation (Heasley *et al.*, 2000). Samples with well-developed isopachous rims were relatively more resistant to mechanical and chemical compaction than those without rims. Elsewhere, syntaxial growths prevented compaction of echinoid bioclast particles, but were not sufficiently abundant to prevent the development of chemical compaction in the surrounding ooids (Heasley *et al.*, 2000). Microporosity in the ooids was apparently generated by dissolution subsequent to chemical compaction (Heasley *et al.*, 2000). Many carbonate reservoirs have been shown to contain secondary diagenetic burial porosity, although their distribution is restricted (Giles & Marshall, 1986; Mazzullo & Harris, 1991). Dissolution of deep burial would require the introduction of acidic and/or undersaturated fluids from outside the reservoir (Heasley *et al.*, 2000). CO_2 and organic acids from kerogen maturation are released into aqueous pore fluids expelled from source rocks during initial petroleum generation (Hunt, 1996). Another alternative explanation is based on the backward solubility of calcite with respect to temperature. Tectonic activity in the Tertiary may have provided opportunities for fluid flow from deeper parts of the basin. The aqueous fluids associated with the hydrocarbons may have been saturated with respect to calcite in depth, but in thermal imbalance with the shallower Albian reservoir, generating dissolution of carbonate particles. (Heasley *et al.*, 2000).

5.4 Reservoir Petrofacies

In this study, nine reservoir petrofacies were defined using the concepts established by De Ros & Goldberg (2007), where the main primary and diagenetic parameters that control the permeability and porosity of the studied samples were identified.

Porous Oolitic Calcarenites (POOCAL): These samples range from fine to coarse sand with a predominance of medium sand texture. They are massive, well-sorted, with normal packing. The primary constituents are predominantly oolites, some polycomposites, oncolites, peloids, rare particulate sand intraclasts and bioclasts of bivalves and gastropods. Siliciclastic grains are rare. The pore system is predominantly interparticle, with moderate to good connectivity between the pores. Intraparticle porosity occurs in oolites and oncolites (Fig. 9 A). The average microporosity is 14.2%, and the average permeability is 0.90 mD.

Porous Oncolitic Calcarenites (PONCAL): These samples vary in texture from medium to very coarse sand, with a predominance of coarse sand. They are poorly sorted rocks, predominantly massive, some fractured. Agglomerated oncolites are common, and microbial and particulate sand intraclasts are rare. The pore system of these rocks has moderate to good connection, with good connectivity between interparticle pores. Intraparticle porosity occurs in oncolites and oolites, and some samples show vugular pores (Fig. 9 B). The average microporosity is 12.3%, and the permeability is 1.06 mD.

Hybrid Arenites (HYARB): These samples are composed of similar proportions of siliciclastic grains and carbonate allochemical particles. They are predominantly of medium sand grain size, massive and with normal packing (Fig. 9 C). The main siliciclastic grains are angular quartz, K-feldspar, biotite and muscovite sub-grains, mixed with oolites, peloids, oncolites and bioclasts. The pore system has a moderate connection, and some samples show moderate interparticle porosity. Intraparticle porosity is common in bivalve bioclasts, oolites, and feldspar grains. The average microporosity is 4.6%, and the average permeability is 4.5 mD.

Cemented Oolitic Calcarenites (CEOOCAL): These samples vary in texture from fine to coarse sand, with a predominance of medium sand. They are rocks with a massive structure, well sorted, and with normal packing. Some samples have polycomposite oolites. Interparticle porosity has been partially destroyed by cementation. Intraparticle porosity occurs in oolites and oncolites, and in some bivalve and gastropod bioclasts (Fig. 9 D). The average microporosity is 5.2%, and the average permeability is 0.10 mD.

Cemented Oncolitic Calcarenites (CEONCAL): These samples vary in texture from fine sand to predominantly coarse sand. They are massive, poorly sorted rocks with normal packing. The pore system of these samples is poorly connected. Interparticle porosity has been reduced by cementation. Fracture pores are rare. Intraparticle porosity occurs in oncolites and bivalve bioclasts. The average macroporosity is 4.5%, and the permeability is 4.7 mD.

Cemented Oncolitic Calcirrudites (CEONCR): These samples vary in texture from medium to pebble, with a predominance of coarse sand. They are poorly sorted, massive rocks, some locally fractured. The pore system of these rocks is poorly connected. Primary interparticle porosity is reduced due to cementation and compaction. Intraparticle porosity occurs in oncolites and bivalve bioclasts. The average microporosity is 4.5%, the average permeability is 0.91 mD.

Compacted Peloid Calcarenites (COMPECA): These samples vary texturally from fine to predominantly medium sand, locally fractured and stylolitized. The pore system is poorly connected (Fig. 9 E). Interparticle porosity has been greatly reduced by compaction. The average microporosity is 4.3%, and the average permeability is 0.31 mD.

Compacted Oncolitic Calcarenites (COMONC): These samples have a predominant medium sand grain size, are poorly sorted, fractured and stylolitized. Interparticle porosity was reduced by compaction, and intraparticle porosity was observed in dissolution of oncolites, and bioclasts of bivalves and gastropods. The average microporosity is 5.1%, and the average permeability is 2.11 mD.

Compacted Oncolitic Calcirrudites (COMONCR): These samples are very poorly sorted, with a predominant textural size of coarse sand, tight packing, fractured and stylolitized. The pore system is poorly connected due to cementation and intense compaction (Fig. 9 F). Interparticle porosity is low and intraparticle porosity occurs in oncolites, oolites and bioclasts, with rare vugular pores. The average microporosity is 2.1%, and the average permeability is 0.33 mD.

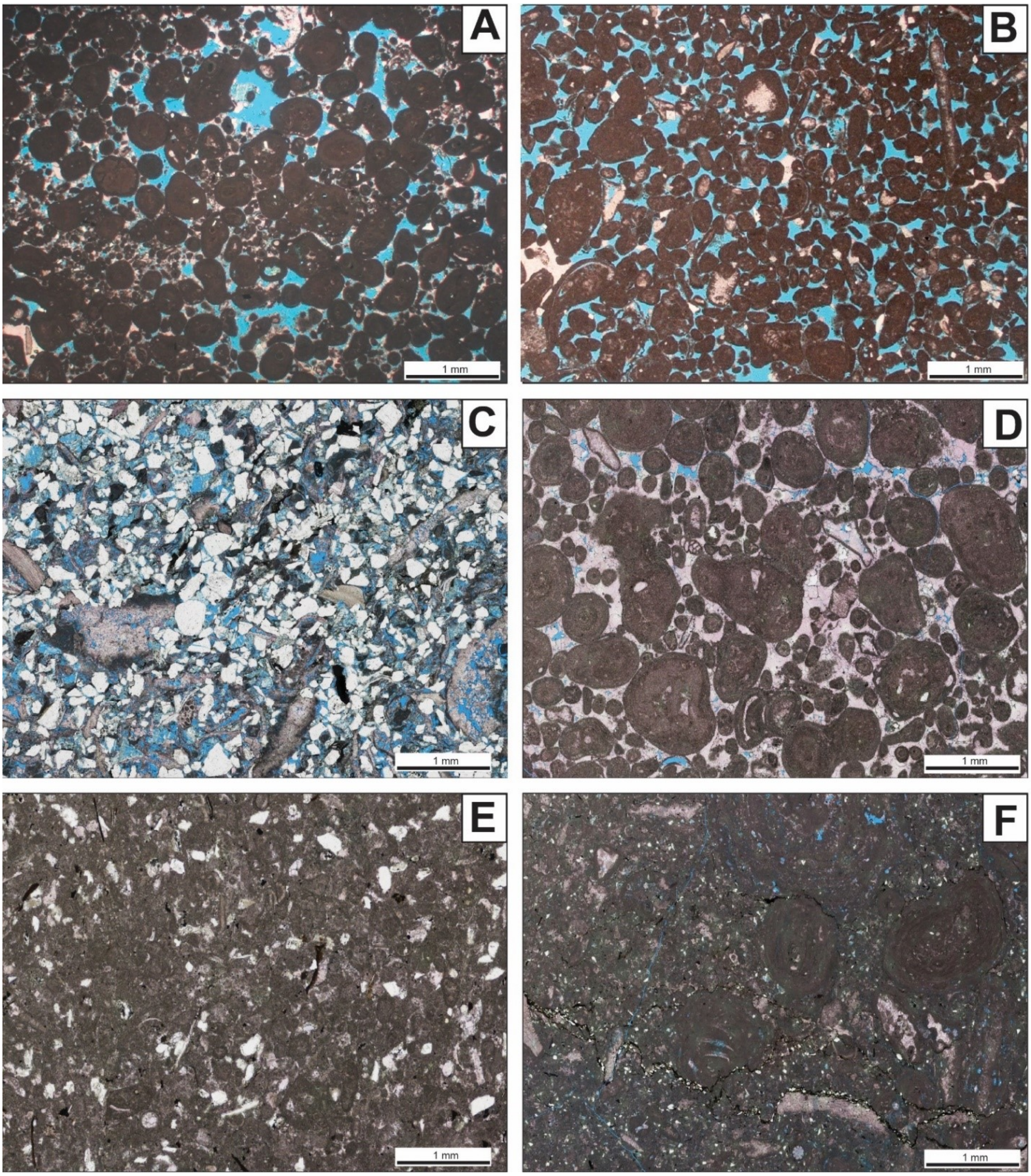

Figure 9. Petrographic characteristics of the main reservoir petrofacies of the Quissamã Formation: A) POOCAL: good quality reservoir petrofacies, with preserved primary interparticle porosity. //P B) PONCAL, good quality reservoir petrofacies, with preserved primary interparticle porosity. //P C) HYARB: medium quality reservoir petrofacies due to dissolution of bioclasts and feldspars. //P D) CEOOCAL: poor quality reservoir petrofacies, with reduced porosity by calcite cementation. //P. E) COMPECA: non-reservoir, due to intense compaction. //P. F) COMONCR: poor quality reservoir petrofacies, due to intense compaction. //P.

Figura 9. Características petrográficas nas principais petrofácies de reservatório da Formação Quissamã: A) POOCAL: petrofácies de reservatório de boa qualidade, com porosidade interpartícula primária preservada. //P B) PONCAL, petrofácies de reservatório de boa qualidade, com porosidade interpartícula primária preservada. //P C) HYARB: petrofácies de reservatório de qualidade média devido à dissolução de bioclastos e feldspatos. //P D) CEOCOCAL: petrofácies de reservatório de má qualidade, com porosidade reduzida pela cimentação por calcita. //P. E) COMPECA: não-reservatório, devido a intensa compactação. //P. F) COMONCR: petrofácies de reservatório de má qualidade, devido a intensa compactação.

5.5 Petrophysical aspects of the Quissamã Formation

Through the Techlog® software, a log-based mineralogical petrophysical data was applied to the logging data of 3-OGX-61-RJS well to define the vertical distribution of the main mineralogical constituents. The modeled constituents are: calcite, dolomite, sílica, and clay minerals (essentially corresponding to feldspars and micas in hybrid samples). Figure 10 shows the used logs, petrophysical and petrographic data, and the result of mineralogical modeling. Track 1 shows the gamma-ray (green line) and caliper (brown line) curves. Tracks 2 and 3 shows the depth and cored interval, respectively. Track 4 shows the resistivity, and track 5 the density (black line). The model also compares the total and effective porosity, calculated with the density profiles, with the petrographic porosity (track 6, red line). Tracks 10 to 15 show the calculated mineralogical values.

A good correspondence is observed between the mineralogical model built in Techlog and the petrographic results for the studied well (points plotted next to the graphs). Petrophysical porosity and permeability data show a good correlation (Figure 11), with a group of samples with good porosity (> 10%) and permeability (> 1 mD; Figure 10 yellow plots), with good pore connectivity and a large volume of interparticle porosity, another with low permeability (< 1 mD) and good porosity (> 10%), corresponding to rocks with moldic, intraparticle and channel pores, and a last group with low permeability (< 1 mD) and low porosity (< 10 %), corresponding to very cemented or severely compacted rocks (Fig.10 red plots).

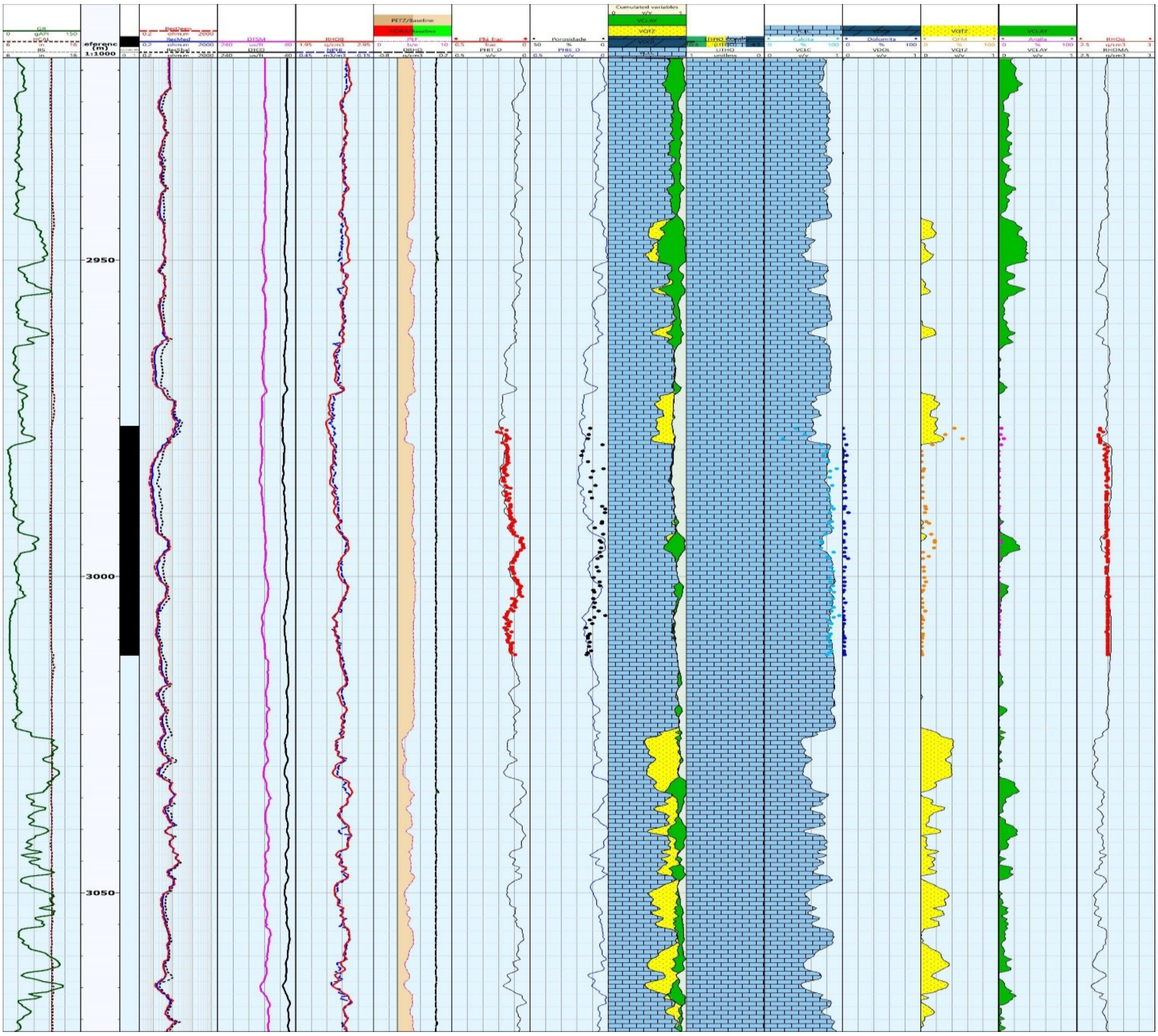

Figure 10: Log signatures and petrophysical analyses of the lower Albian section in well 3-OGX-61-RJS. 1- Gamma rays (green line) and Caliper (dashed brown line). 2 - Measured depth. 3- Cored interval. 4- Deep Resistivity (dashed red line), Medium Resistivity (solid blue line), and Shallow Resistivity (dotted black line). 5 - Sonic recordings of Compressional (black line) and Shear (pink line) waves. 6- Density (red line) and Neutrons (dashed blue line). 7- Photoelectric factor (dotted pink line) and Density correction (dashed black line). 8- Total porosity (solid black line) and petrophysical porosity (red points). 9- Effective porosity (solid blue line) and petrographic porosity (black points). 10 to 15- Calculated mineralogical profiles and petrographic data. Profile of Calcite (blue), Silica (yellow), and Clay (green). Petrographic contents of calcite (light blue points), dolomite (dark blue points), silicates (orange points), and clay (pink points). 16- Calculated matrix density (black line) and grain density measured in the laboratory (red points).

Figura 10. Assinaturas de perfis e análises petrofísicas da seção do Albiano inferior no poço 3-OGX-61-RJS. 1- Raios gama (linha verde) e Cáliper (linha marrom tracejada). 2- Profundidade medida. 3- Intervalo testemunhado. 4- Resistividade Profunda (linha vermelha tracejada), Resistividade Média (linha azul contínua) e Resistividade rasa (linha preta pontilhada). 5- Registros sônicos das ondas Compressional (linha preta) e Cisalhante (linha rosa). 6- Densidade (linha vermelha) e Nêutrons (linha azul tracejada). 7- Fator fotoelétrico (linha rosa pontilhada) e Correção da densidade (linha preta tracejada). 8- Porosidade total (linha preta contínua) e Porosidade petrofísica (pontos vermelhos). 9- Porosidade efetiva (linha azul contínua) e Porosidade petrográfica (pontos pretos). 10 a 15- Perfis mineralógicos calculados e dados petrográficos. Perfil de Calcita (azul), Sílica (amarelo) e Argila (verde). Teores petrográficos de calcita (pontos azuis claros), dolomita (pontos azuis escuros) e silicatos (pontos laranja), argila (pontos rosa). 16- Densidade da matriz calculada (linha preta) e Densidade de grãos medida em laboratório (pontos vermelhos).

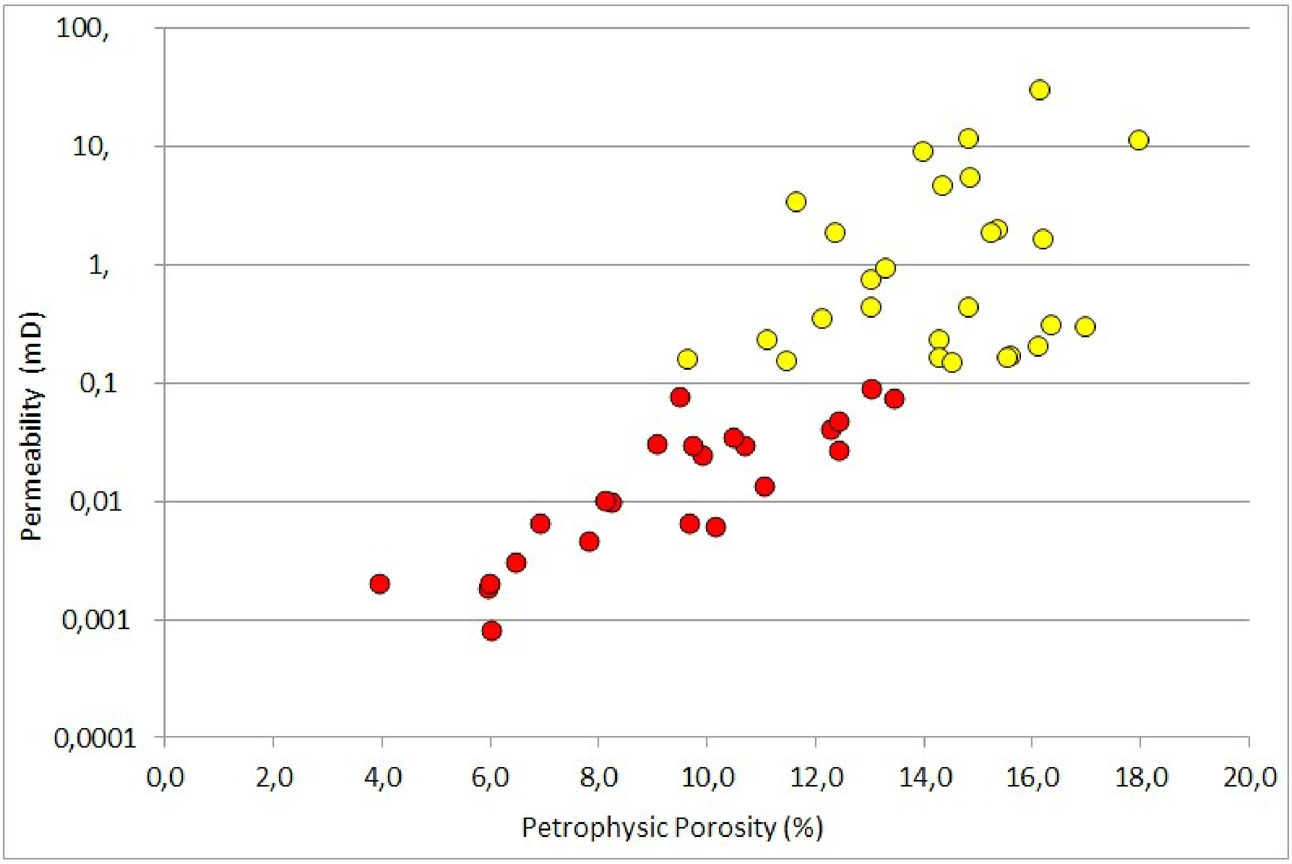

Figure 11. Plot of petrophysical porosity x permeability of the studied Quissamã samples.

Figura 11. Gráfico de porosidade petrofísica x permeabilidade das amostras da Formação Quissamã.

5.6 Reservoir quality of the Quissamã Formation

The reservoir quality of the studied rocks of the Quissamã Formation was defined based on the primary composition, texture, and mainly on the diagenetic processes and products with the greatest impact on the porosity and permeability defined in the nine reservoir petrofacies observed (Table 11).

The POOCAL (Porous Oolitic Calcarenites) and PONCAL (Porous Oncolitic Calcarenites) petrofacies have good reservoir quality. These two petrofacies were deposited in high- and moderate-energy environments, respectively, and show good preservation of primary interparticle porosity due to partial eodiagenetic cementation by calcite and limited mechanical and chemical compaction. The pore system of these petrofacies has good connectivity. Eodiagenetic cementation by calcite rims and syntaxial growths on echinoids helped to support the framework of these rocks, inhibiting the effects of compaction. Although calcite cementation reduced the pore throats, the connectivity of the pore system was only partially affected, and their permeability and microporosity correspond to good reservoirs. Secondary porosity generation was limited to a few intraparticle pores in ooids, oncoids, and carbonate sand intraclasts, with rare moldic and vugular pores that do not contribute significantly to reservoir quality (Fig. 12).

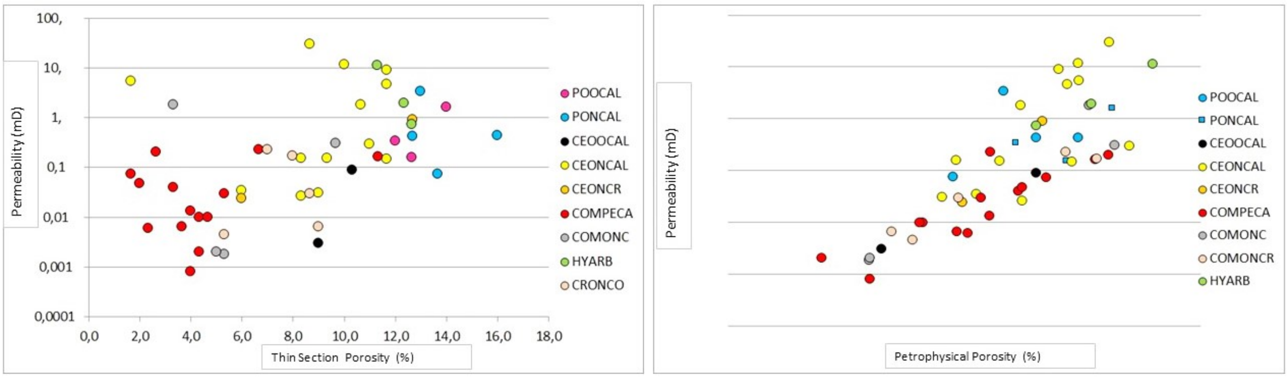

Figure 12. Plots of permeability versus petrophysical porosity and thin section porosity for defined petrofacies.

Figura 12. Gráficos de permeabilidade versus porosidade petrofísica e porosidade petrográfica para as petrofácies definidas.

Table 11. Average values of Macroporosity, Microporosity, Permeability and Reservoir Quality classification for the petrofacies recognized in the studied samples.

Tabela 11. Valores médios de Macroporidade, Microporosidade, Permeabilidade e Qualidade de reservatório para as petrofácies reconhecidas nas amostras estudadas.

Petrofacies	Macroporosity (%)	Microporosity (%)	Permeability (mD)	Quality
POOCAL	13.6	14.2	0.9	Good
PONCAL	8.6	12.3	1.6	Good
HYARB	2.7	4.6	4.5	Moderate
CEOOCAL	2.9	5.2	0.10	Poor
CEONCAL	4.9	4.5	4.7	Moderate
CEONCR	3.3	4.5	0.9	Poor
COMPECA	5.1	4.3	0.3	Non-reservoir
COMONC	4.4	5.1	2.1	Non-reservoir
COMONCR	3.2	2.1	0.3	Non-reservoir

The Hybrid arenites petrofacies (HYARB) have a regular reservoir quality, with some preservation of intergranular porosity and limited calcite cementation, with some kaolinite replacing feldspars and filling dissolution pores of some feldspar grains. Mechanical compaction is visible in some fractured feldspar and bioclasts, and some samples have a fair connection between the pores, with reasonable permeability. Secondary porosity was generated by the dissolution of oncoids, ooids, bivalve bioclasts and feldspars.

The cemented petrofacies CEOOCAL, CEONCAL and CEONCR (cemented oolitic/oncolitic calcarenites and calcirrudites), were deposited in moderate to high energy environments, and have low reservoir quality, due to intense carbonate cementation. These rocks display limited compaction due to the early cementation, but strong reduction in porosity and permeability. In these samples, both the primary interparticle porosity, as well as the intraparticle and moldic porosity formed by particle dissolution, were practically obliterated by mosaic calcite cement, and less commonly by blocky dolomite.

The compacted petrofacies COMPECA, COMONC and COMONCR (compacted peloidal calcarenites, compacted peloidal oncolitic calcarenites and compacted peloidal oncolitic calcirudites) were deposited in moderate energy environments, and constitute the worst reservoir quality among the samples analyzed, classified as non-reservoirs. The main mechanism for porosity reduction in these samples was the mechanical and chemical compaction. The minor eodiagenetic cementation was unable to support the framework of these rocks against compaction. Secondary porosity is limited, and intraparticle and moldic pores are isolated and unconnected. The only permeability observed in these compacted petrofacies was promoted by the burial dissolution along stylolites, forming vugular and channel pores, and by fractures.

6. Conclusions

An integrated study using petrographic, sedimentological, petrophysical, and log data was carried out to improve the understanding of the factors that control the origin, evolution, and distribution of porosity in the carbonate rocks of the Quissamã Formation in 3-OGX-61-RJS well. The main conclusions are listed below:

- Six depositional facies were identified in the analyzed well, grouped into two facies associations: moderate-energy intermediate carbonate ramp and high-energy shallow carbonate ramp. The lithologies comprise: oolitic calcarenites/calcirudites characteristic of a high-energy environment, deposited in the crest of elongated shoals, intercalated with oncolitic and peloidal calcarenites/calcirudites deposited in moderate energy environments along the shoal flanks.
- The main diagenetic products and processes identified are: micritization of allochemical particles, microcrystalline and framboidal pyrite replacing particles, cementation by calcite rims, mosaic calcite and syntaxial growths on echinoid bioclasts, particle dissolution and generation of secondary porosity, authigenesis of kaolinite, mechanical compaction, cementation by blocky dolomite, chemical compaction generating stylolites and sutured interparticle contacts, saddle dolomite, mesodiagenetic dissolution, calcite filling dissolution pores.
- The pore system is heterogeneous, the primary composition and the eodiagenetic and mesodiagenetic processes that affected the reservoir. Cementation and compaction were the diagenetic processes that most impacted the quality of the reservoirs.
- Nine reservoir petrofacies were defined based on the integration of petrographic and petrophysical data and the features that most impacted the permeability and porosity. The best petrofacies are porous oolitic and oncolitic calcarenites, which have a good connection of preserved interparticle porosity and limited early cementation that preserved the framework from the effects of compaction. The worst petrofacies are peloidal

calcarenites and calcirudites that were very cemented or very compacted, characterized as non-reservoirs.

- Diagenesis was the main factor controlling the quality of the studied Albian reservoirs. The variation in the intensity of the cementation, compaction and dissolution processes directly impacted the pore systems. The depositional environment had proportionally little influence on the quality of the reservoirs, as rocks deposited in moderate energy environments constitute good quality reservoirs.
- Two secondary porosity generation events occurred in the studied samples: the first event occurred during eodiagenesis, with the generation of moldic, vugular and intraparticle pores in ooids, oncoids and less frequently in bioclasts and peloids. This dissolution was generated by the influx of meteoric fluids during episodic exposure of the carbonate shoals. The second event of secondary porosity generation was generated during mesodiagenesis, with dissolution by evolved fluids along stylolites and fractures, forming channel pores and micropores through the dissolution of grains and cements close to these structures.
- The better understanding of the factors and processes that affected the porosity of the Albian carbonate rocks of the Quissamã Formation shall contribute to predict the reservoir quality in exploration areas, as well as to increase recovery efficiency from producing fields.

Acknowledgments: The authors gratefully acknowledge support from Shell Brasil Petróleo Ltda. through the project: Multidisciplinary Integrated Study of the Albian in the Santos, Campos and Espírito Santo Basins, project at COPPE/UFRJ and UFRGS. We thank Solintec for the access to samples and data as well as to acknowledge the strategic importance of the support given by ANP through the R&D levy regulation

Contributions from Authors: Leonardo Morejano Halfen: Conceptualization; Formal analysis, Methodology; Validation; Writing – original draft; Luiz Fernando De Ros: Writing review and editing; Supervision; Visualization; José Alves Luís Drummond Alves: Supervision; Visualization. Francyne Bochi do Amarante: Methodology; Visualization. Gisela Miranda de Souza Almeida: Methodology Todos os autores leram e concordaram com a versão publicada do manuscrito".

Conflict of interest: There is no conflict of interest or competing interests.

References

Amarante, F.B.; Jackson, C.A.; Pichel, L.M.; Scherer, C.M.S.; Kuchle, J. 2021. Pre-salt rift morphology controls salt tectonics in the Campos Basin, offshore SE Brazil. *Basin Research*, 33(5): 2837-2861. https://doi.org/10.1111/bre.12588

ANP - Agência Nacional do Petróleo 2024. *Boletim da produção de petróleo e gás natural*. https://www.gov.br/anp/pt-br/centrais-de-conteudo/publicacoes/boletinsanp/boletins/arquivos-bmppgn/2024/boletim-setembro.pdf

Armelenti, G.; Goldberg, K.; Alvarenga, R.; Kuchle, J.; Amarante, F.B.; Scherer, C.M.S.; Bastos, A.C; Conceição, J.C.; Alves J.L.D.; De Ros, L.F. 2021. Depositional and diagenetic impacts on the porosity of post-salt carbonate reservoirs of southern Campos Basin, southeastern Brazilian margin. *Journal of South American Earth Sciences* 112(1): 103566. https://doi.org/10.1016/j.jsames.2021.103566

Azevedo, R. L. M. 2004. Paleoceanografia e a evolução do Atlântico Sul no Albiano. *Boletim de Geociências da Petrobras, v. 12, p. 231-249.*

Berner, R.A. 1984. Sedimentary pyrite formation: An update. *Geochimica et Cosmochimica Acta* 48(4): 605-615. https://doi.org/10.1016/0016-7037(84)90089-9

Bliefnick, D.M. & Kaldi, J.G. 1996. Pore Geometry: Control on Reservoir Properties, Walker Creek Field, Columbia and Lafayette Counties, Arkansas. *AAPG Bulletin* 80(7): 1027-1044. https://doi.org/10.1306/64ED8C82-1724-11D7-8645000102C1865D

Bramkamp, R.A. & Powers, R.W. 1958. Classification of Arabian carbonate rocks. *Bulletin of the Geological Society of America* 69(10): 1305-1308. https://doi.org/10.1130/0016-7606(1958)69[1305:COACR]2.0.CO;2

Bruhn, C.H.L.; Gomes, J.A.T.; Lucchese, C.D.; Johann, P.R.S. 2003. Campos Basin: reservoir characterization and management - Historical overview and future challenges. *Paper OTC 15220 presented at the Offshore Technology Conference*, Houston, Texas 14 p.

Carozzi, A.V.; Falkenhein, F.U.H., Franke, M.R. 1983. Depositional environment, diagenesis and reservoir properties of oncolitic packstones, Macaé Formation (Albian-Cenomanian), Campos Basin, offshore Rio de Janeiro, Brazil. In: Peryt, T. M. (Eds.), *Coated Grains*. Springer-Verlag, Berlin, Heidelberg, p. 330-343. https://doi.org/10.1007/978-3-642-68869-0_28

Carvalho, M.D. 2002. Stratigraphic control on facies, diagenesis and porosity development of dolomitized oolitic-oncolitic ramp sequence in Macaé Formation, Campos Basin, Brazil. 16th International Sedimentological Congress, *Abstracts Volume (2002)*, p. 63.

Choquette, P.W. & Pray, L.C. 1970. Geologic nomenclature and classification of porosity in sedimentary carbonates. *AAPG Bulletin* 54(2): 207-250. https://doi.org/10.1306/5D25C98B-16C1-11D7-8645000102C1865D

De Ros, L.F. & Goldberg, K. 2007. Reservoir petrofacies: a tool for quality characterization and prediction. In: AAPG Annual Conference and Exhibition, 1-4 April, Long Beach, USA, *Extended Abstracts*, 6.

De Ros, L.F.; Goldberg, K.; Abel, M.; Victorinetti, F.; Mastella, L.; Castro, E. 2007. Advanced acquisition and management of petrographic information from reservoir rocks using the PETROLEDGE® System. In: AAPG Annual Conference and Exhibition, 1-4 April, Long Beach, USA, *Extended Abstracts*, 6.

Dickson, J. A. 1965 Modified Staining Technique for Carbonates in Thin Section. *Nature* 205, 587. https://doi.org/10.1038/205587a0

Dias, J.L.; Scarton, J.C.; Esteves, F.R.; Carminatti, M.; Guardado, L.R. 1990. Aspectos da evolução tectono-sedimentar e a ocorrência de hidrocarbonetos na Bacia de Campos. In: Gabaglia, G.P.R., Milani, E.J. (Eds.), *Origem e evolução de bacias sedimentares*. Petrobras, p. 333-360.

Falkenhein, F.U.H.; Franke, M.R.; Carozzi, A.V. 1981. Petroleum Geology of the Macaé Formation (Albian-Cenomanian), Campos Basin, Brazil (Carbonate Microfacies, Depositional and Diagenetic Models-natural and Experimental Porosity). *Ciência, Tecnologia e Pertróleo* 11, 140 pp.

Favoreto, J.; Rohn, R.; Lykawa, R.; Okubo, J. 2016. Caracterização sedimentológica dos carbonatos Albianos do reservatório Quissamã na porção meridional da Bacia de Campos. *Revista Brasileira de Geociências* 35(1): 1-15. http://hdl.handle.net/11449/172816

Figueiredo, A.M.F. & Mohriak, W.U. 1984. A tectônica salífera e as acumulações de petróleo da Bacia de Campos. in: *XXXIII CONGRESSO BRASILEIRO DE GEOLOGIA*, 1984, SBG, p.1380-1394

Giles, M.R. & Marshall, J.D. 1986. Constraints on the development of secondary porosity in the subsurface: re-evaluation of processes. *Marine Petroleum Geology* 3(3): 243-255. https://doi.org/10.1016/0264-8172(86)90048-6

Giles, M.R. & De Boer, R.B. 1989. Secondary porosity: creation of enhanced porosities in the subsurface from the dissolution of carbonate cements as a result of cooling formation waters. Marine and Petroleum Geology 6(3): 261-269. https://doi.org/10.1016/0264-8172(89)90005-6

Grabau, A.W. 1904. On the classification of sedimentary rocks. *American Petroleum Geologists AAPG*, 33: 228-247.

Guardado, L.R.; Gamboa, L.A.P.; Lucchesi, C.F. 1989. Petroleum Geology of the Campos Basin, a Model for a Producing Atlantic-Type Basin. In: Edwards J.D. & P.A. Santogrossi (Eds.), *Divergent/Passive Margin Basins: AAPG Memoir 48*, p.3-79. https://doi.org/10.1306/M48508C1

Heasley, E.C.; Worden, R.H.; Hendry, J.P. 2000. Cement distribution in a carbonate reservoir: recognition of a palaeo oil water contact and its relationship to reservoir quality in the Humbly Grove field, onshore, UK. Marine and Petroleum Geology 17(5): 639-654. https://doi.org/10.1016/S0264-8172(99)00057-4

Hunt, J.M. 1996. *Petroleum geochemistry and geology*. New York: Freeman and Co 743p.

Longman, M.W. 1980. Carbonate Diagenetic Textures from Nearsurface Diagenetic Environments. *AAPG Bulletin* 64(4): 461-487. https://doi.org/10.1306/2F918A63-16CE-11D7-8645000102C1865D

Machel, H. G.2001 Bacterial and thermochemical sulfate reduction in diagenetic settings. *Sedimentary Geology*, 140: 143-175. https://doi.org/10.1016/S0037-0738(00)00176-7

Machel, H.G. 2004.Concepts and models of dolomitization: a critical reappraisal. In: Braithwaite, C.J.R., Rizzl, G. & Darke, G. (Eds.), *The Geometry and Petrogenesis of Dolomite Hydrocarbon Reservoirs*. Geological Society, London, Special Publication 235, p. 7-63. https://doi.org/10.1144/GSL.SP.2004.235.01.02

Mazzulo, S.J. & Harris, P.M. 1991. An overview of dissolution porosity development in the deep-burial environment, with examples from carbonate reservoirs in the Permian basin. In: Candellaria, M.P. (Ed.), *Permian Basin Plays: Tomorrow`s Techonology Today*. West Texas Geological Society Publication, p. 125-138.

Moore, C.H. & Wade, W.J. 2013. *Carbonate Reservoirs: Porosity and Diagenesis in a Sequence Stratigraphic Framework*. Amsterdam, Elsevier, 392 p.

Morad, D.; Nader, F.H.; Gasparrini, M.; Morad, S.; Rossi, C.; Marchionda, E.; Al Darmaki, F.; Martines, M.; Hellevang, H. 2018. Comparison of the diagenetic and reservoir quality evolution between the anticline crest and flank of an Upper Jurassic carbonate gas reservoir, Abu Dhabi, United Arab Emirates. *Sedimentary Geology*, 367: 96-113. https://doi.org/10.1016/j.sedgeo.2018.02.008

Okubo, J, Lykawka, R., Warren, L.V., Favoreto, J., Dias-Brito, D. 2015. Depositional, diagenetic and stratigraphic aspects of Macaé Group carbonates (Albian): Example from an oilfield from Campos Basin. *Brazilian Journal of Geology*, 45, 243-258. https://doi.org/10.1590/23174889201500020005

Paganoni, M.; Harthi, A.A.; Morad, D.; Morad, S.; Ceriani, A.; Mansurbeg, H.; Suwaidi, A.A.; Al-Aasm, I.S.; Ehrenberg, S.N.; Sirat, M. 2016. Impact of stylolitization on diagenesis of a Lower Cretaceous carbonate reservoir from a giant oilfield, Abu Dhabi, United Arab Emirates. *Sedimentary Geology* 335: 70-92. https://doi.org/10.1016/j.sedgeo.2016.02.004

Rankey E.C.; Riegl B.; Steffen K. 2006. Form, function and feedbacks in a tidally dominated ooid shoal, Bahamas. *Sedimentology* 53: 1191-1210. https://doi.org/10.1016/j.sedgeo.2016.02.004

Robaina, L.E.S.; Formoso, M.L.L.; Spadini A.R. 1993. Geoquímica dos reservatórios carbonáticos da Formação Macaé (Eo-meso- Albiano) nos campos de Pampo e Enchova, Bacia de Campos, Brasil. *Boletim de Geociências da Petrobras* 7: 103-133.

Sellwood, B.W. & Beckett, D. 1991. Ooid microfabrics: the origin and distribution of high intra-ooid porosity; Mid Jurassic reservoirs, southern England. *Sedimentary. Geology* 71(3–4): 189-193. https://doi.org/10.1016/0037-0738(91)90101-I

Spadini, A.R. 1992. *Processos deposicionais e ciclicidade em carbonatos albianos da plataforma rasa da Bacia de Campos*. Universidade Federal do Rio de Janeiro, 143p. Dissertação de Mestrado

Spadini, A.R.; Esteves, F.R.; Dias-Brito, D.; Azevedo, R.L.M.; Rodrigues, R. 1988. The Macaé Formation, Campos Basin, Brazil: Its evolution in the context of the initial history of the South Atlantic: *Revista Brasileira de Geociências* 18: 261-272.

Spötl, C. & Pitman, J. 1998. Saddle (baroque) dolomite in carbonates and sandstones: a reappraisal of a burial-diagenetic concept. In: S. Morad (Ed.), Carbonate Cementation in Sandstones: Distribution Patterns and Geochemical Evolution. IAS Special Publication 26, p. 437-460. https://doi.org/10.1002/9781444304893

Tucker, M.E. 1988. *Techniques in Sedimentology*. Oxford, Blackwell Scientific Publication, 391p.

Tucker, M.E. & Wright, V.P. 1990. *Carbonate Sedimentology*. England, Oxford, Blackwell Science, 492 p.

Winter, W.R.; Jahnert, R.J.; França, A.B. 2007. Bacia de Campos. *Boletim de Geociências da Petrobras* 15: 511-529.

Worden, R.H. & Morad, S. 2003. Clay minerals in sandstones: Controls on formation, distribution and evolution. In: Warden, R.H.; Morad, S. (Eds.), Clay Mineral Cements in Sandstones: Oxford, International Association of Sedimentologists 34: 3-41. https://doi.org/10.1002/9781444304336.ch1

Zuffa, G.G. 1980. Hybrid arenites. Their composition and classification. *Journal of Sedimentary Petrology* 50: 21-29. https://doi.org/10.1306/212f7950-2b24-11d7-8648000102c1865d